Regional-scale 3D modelling in metamorphic belts: An implicit model-driven workflow applied in the Pennine Alps

Gloria Arienti, Andrea Bistacchi, Guillaume Caumon, Giovanni Dal Piaz, Bruno Monopoli, Davide Bertolo

▶ **To cite this version:**

Gloria Arienti, Andrea Bistacchi, Guillaume Caumon, Giovanni Dal Piaz, Bruno Monopoli, et al.. Regional-scale 3D modelling in metamorphic belts: An implicit model-driven workflow applied in the Pennine Alps. Journal of Structural Geology, 2024, pp.105045. 10.1016/j.jsg.2023.105045 . hal-04388453

HAL Id: hal-04388453
https://hal.science/hal-04388453

Submitted on 11 Jan 2024

HAL is a multi-disciplinary open access archive for the deposit and dissemination of scientific research documents, whether they are published or not. The documents may come from teaching and research institutions in France or abroad, or from public or private research centers.

L'archive ouverte pluridisciplinaire **HAL**, est destinée au dépôt et à la diffusion de documents scientifiques de niveau recherche, publiés ou non, émanant des établissements d'enseignement et de recherche français ou étrangers, des laboratoires publics ou privés.

Distributed under a Creative Commons Attribution - NonCommercial - NoDerivatives 4.0 International License

Author's version published in Journal of Structural Geology, January 2024, 105045 10.1016/j.jsg.2023.105045 –
CC-BY-NC-ND

Regional-scale 3D modelling in metamorphic belts: an implicit model-driven workflow applied in the Pennine Alps

*Gloria Arienti[a], Andrea Bistacchi[a], Guillaume Caumon[b,c], Giovanni DAL PIAZ[d], Bruno Monopoli[d] and Davide Bertolo[e]

[a] Dipartimento di Scienze dell'Ambiente e della Terra, Università degli Studi di Milano-Bicocca, 20126 Italy

[b] RING, GeoRessources - ENSG, Université de Lorraine - CNRS, 54000 France

[c] Institut Universitaire de France (IUF)

[d] LTS s.r.l., Treviso, 31020 Italy

[e] Regione Autonoma Valle d'Aosta, Dipartimento Programmazione, Risorse Idriche e Territorio, 11100 Italy

Corresponding author's contact details:

gloria.arienti@unimib.it | Italy 0039 0264484061 | Piazza della Scienza, 4, 20126 Milano, Italy

Keywords

3D implicit modelling | regional 3D model | metamorphic mountain belt | North-Western Alps | Alpine tectonic contacts | Pennine Alps

Abstract

Leveraging a high resolution geological and structural dataset acquired over decades of fieldwork, we build the 3D structural model of a portion of the highly deformed core of the Alpine orogen, in the Northern Aosta Valley. The model represents tectonic contacts separating the tectono-metamorphic units outcropping along the section between Mont Blanc and Monte Rosa, and it covers an area of ca. 1,500 km^2. The input source data include original 1:10,000 geological surveys synthetised in a 1:75,000 tectonic map, and a dense database of structural stations. After a first orientation statistics study of the structural field database, our workflow develops through structural interpretation in vertical cross-sections that allow including in the modelling process structural drivers such as crosscutting relationships, interference patterns, kinematic constraints and fold morphology from detailed field studies. Three-dimensional interpolation on a tetrahedral mesh using the implicit Discrete Smooth Interpolator method follows, using also foliation and fold axes data as interpolation constraints. After describing the workflow and the model, we discuss the difficulties of modelling in polydeformed metamorphic complexes. In particular, we address the issue of modelling shear zones, refolded, isoclinal and/or recumbent folds and dense networks of faults, that characterise the geology of the Northern Aosta Valley.

1. Introduction

Three-dimensional modelling of geological structures plays an essential role in the investigation and quantification of geological and tectonic processes in space and time. The importance of 3D modelling has been established in the past decades with applications in a variety of fields, from oil and gas (e.g., Kroeger et al., 2019), mining (e.g., Sides, 1997; Vollgger et al., 2015) and geothermal exploration (e.g., Milicich et al., 2018). Three-dimensional models have also been of great importance in geoengineering (e.g., Xiong et al., 2018; Soldo et al., 2022), groundwater projects (e.g., Hassen et al., 2016) and for CO_2 and gas storage studies (e.g., Kaufmann and Martin, 2009; Thanh et al., 2019).

Geological modelling has moreover been used in combination with geophysical inversion for the enforcement of geological realism and to better assess subsurface uncertainty (e.g., Guillen et al., 2008; Giraud et al., 2023; Liang et al., 2023; Jessell et al., 2010; Caumon, 2010).

Methods used to model the geological structures in three-dimensional space can be categorised into two first-order classes: data-driven and model-driven approaches (Wellmann and Caumon, 2018). Data centric methods retrieve physical properties from large geophysical datasets (e.g., geophysical imaging or borehole measurements), then interpret these data as geological features of interest (Wellmann and Caumon, 2018). On the other hand, model-driven approaches (also referred to as knowledge-driven approaches) revolve around geological conceptual models built based on a priori identification of geological objects and their associated knowledge (Perrin et al., 2005).

In the broad framework of model-driven approaches, another fundamental distinction must be made between explicit and implicit representations. Explicit surface modelling consists in directly building geological interfaces as triangulated surfaces or regular 2D grids by interpolating input data, with each node of the surface characterised by its x, y, z position in 3D (Caumon et al., 2009). However, this class of methods may involve significant expert input from the interpreter (Caumon et al., 2009; Wellmann and Caumon, 2018) when it comes to complexly folded tectonic settings, unconformities and finite internal faults (i.e., faults with a finite area that have the tip line within the modelling domain), requiring considerable expert working time to reach an acceptable modelling outcome.

On the other hand, implicit surface approaches exploit the analogy between a generalised geological "time", as recorded in stratified formations, and a continuous and derivable (excepts at faults and unconformities) scalar field (Houlding, 1994). The whole 3D volume is modelled all at once, from prior information about stratigraphic units, faults and unconformities, to build a continuous scalar field from which stratigraphic surfaces can be extracted as equipotential implicit isosurfaces or level sets. From the first mathematical definitions of this approach (Mallet, 1988; Houlding, 1994; Lajaunie et al., 1997), many steps have been taken towards the integration of geological information into the scalar field, enhancing the mathematical constraints that guide the interpolation of structural field data in the three-dimensional volume (Frank et al., 2007; Calcagno et al., 2008; Hillier et al., 2013; Laurent, 2016) such as fold data (Hillier et al., 2014; Laurent et al., 2016; Grose et al., 2017) and faults (Laurent et al., 2013; Godefroy et al., 2018).

Furthermore, implicit interpolation methods fall into two categories: meshless and mesh-based methods. Meshless approaches use Radial Basis Function interpolators (Carr et al., 2001; Hillier et al., 2014), dual kriging methods (Calcagno et al., 2008; De La Varga et al., 2019) or point-based moving least squares basis functions (Renaudeau et al., 2019). They benefit from a mathematical formulation that does not require a mesh, but their implementation results in a dense system of equations of size $\sim N^2$, where N is the number of data (or interpolation) points, that may become unmanageable even by modern workstations when N is large (in medium-sized models it is common to have $N > 10{,}000$). On the other hand, mesh-based interpolation algorithms work on tetrahedral (Frank et al., 2007; Caumon et al., 2013; Irakarama et al., 2022) or Cartesian (Irakarama et al., 2018) meshes, whose computational complexity and memory weight generally scale linearly with the mesh size, hence can be easily tuned by changing the mesh resolution.

Most of the methods mentioned above have been developed to specifically address the representation of gently deformed sedimentary sequences in tectonic settings on which the attention of the oil-and-gas exploration is focused (e.g., Mallet, 2014). Consequently, dealing with complex structures in basement and cover metamorphic units employing implicit methods remains a major challenge. Geometries such as polyphasic isoclinal and/or recumbent folds, major thrusts and stacks of tectono-metamorphic units, and dense networks of faults concur to the substantial complexity of the geology of metamorphic units in the core of mountain belts, which are a frontier for ambitious 3D structural

modelling projects (de Kemp, 2000; Maxelon and Mancktelow, 2005; Bistacchi et al., 2008; Philippon et al., 2015; Thornton et al., 2018).

To aid the modelling of complex folded geometries, methodologies have been proposed to integrate structural principles (Maxelon et al., 2009; Hillier et al., 2014; Laurent et al., 2016; Grose et al., 2017; Pizella et al, 2022). However, the challenge extends beyond the representation of complex geometries, as the modelling process also involves the upscaling of the often too detailed geological database to align with the model's scale. For this, upscaling strategies for structural data have been proposed (e.g., Carmichael and Ailleres, 2016), overall contributing to the ongoing research for automatic modelling workflows that, if found, would enhance both the reproducibility and efficiency of the modelling process. While such workflows have been proposed for less intricate tectonic settings (Jessell et al., 2021), this remains a topic of active research.

In this paper we use the geomodelling approach to build a 3D regional-scale structural model of the Northern Aosta Valley (ca. 1,500 km^2 of extension in the Italian North-Western Alps), also including a narrow portion of the Swiss territory for the sake of a continuous interpretation. In the framework of the Interreg RESERVAQUA project, the creation of the 3D model is motivated by the development of a programme for sustainable water resource management in relation to climate change. The mountain regions bounding the Alpine belt are heavily dependent on water stored in the mountains in various forms to meet their hydric demand. Information on the distribution of water reserves is therefore crucial, and it is why with our 3D structural model we fill the absence of a three-dimensional representation of this portion of the North-Western Alps. Not less important are the implications on regional tectonic studies of the area, whose interpretation is enhanced and validated by the three-dimensional reasoning allowed by the 3D modelling.

Our model covers the area between the massifs of Mont Blanc (Monte Bianco, 4,808 m a.s.l.) and Monte Rosa (4,634 m a.s.l.) in the Pennine Alps, where a vertical drop of ca. 4,300 m is observed between the highest peaks and the valley floors. This area includes other iconic mountains of the Alps, such as the Grand Combin (4,314 m a.s.l.) and the Monte Cervino (Matterhorn, 4,478 m a.s.l.), deep glacial valleys, high passes such as the Gran San Bernardo (Grand Saint-Bernard, 2,473 m a.s.l.) and a complete sample of tectono-metamorphic units of the core of this collisional mountain belt.

The input dataset is represented by the original 1:10.000 geological maps and related structural data stored within the Geoportale of the Regione Autonoma Valle d'Aosta (https://geoportale.regione.vda.it/), surveyed in the last thirty years for the CARG Project and the Regional Geological Map, mainly by Giorgio V. Dal Piaz (coordinator), Giovanni Dal Piaz, Bruno Monopoli, Alessio Schiavo Andrea Bistacchi, Matteo Massironi and Giovanni Toffolon, with the stratigraphic collaboration of Leonsevero Passeri and Gloria Ciarapica (Dal Piaz et al., 2010, 2016; Perello et al., 2011; Polino et al., 2015). Data are generalised in the tectonic map of Fig. 1.

In the following sections we will summarise the geological and tectonic complexity of the Northern Aosta Valley. Successively, we will describe the steps of our workflow and then the resulting 3D structural model.

2. A summary of the geology of the Northern Aosta Valley

The Alps are a European collisional belt that resulted from the Cretaceous to Present convergence of the Adria continental upper plate and of a subducting lower plate that included a Mesozoic ocean and the continental European lithosphere (Dal Piaz et al., 2003, and references therein). The Penninic-Austroalpine nappe stack, outcropping in the North-Western sector of the Alps, along our study transect, resulted from oceanic subduction, continental collisional and exhumation. It is composed of highly deformed ophiolitic units (Piedmont Zone, remnants of the Mesozoic Tethys Ocean), and continental units from both the European passive margin (Penninic system) and the Adriatic active

margin and related extensional allochthons (Austroalpine system). More external units are the Europe-verging Helvetic and Ultrahelvetic basement slices and decollement cover nappes (marginally represented in our study area) and the Adria-verging Southern Alps (not included in our transect).

The complex structural geology and petrography of units exposed in the Aosta Valley results from superposed Alpine and in some cases Pre-Alpine events. Several relics of Pre-Alpine metamorphic fabrics are still recognised at different scale in basement and pre-Mesozoic rocks. For instance, structures referred to the opening of the Mesozoic ocean are observed in the Piccolo San Bernardo region (Beltrando et al., 2012) and magmatic layering structures are preserved in some Permian gabbroic bodies (Manzotti et al., 2017), while pre-Alpine metamorphic fabrics are mapped from the micro- to the mega-scale in the Valpelline unit of the Dent Blanche Nappe (Gardien et al., 1994). However, more often the present-day structure of the nappe stack reflects Alpine thrusting during lithospheric subduction and continental collision, subsequent extensional deformation related to exhumation of units stacked in the collisional wedge, later uplift and erosion (Dal Piaz et al., 2003).

Detailed structural analysis in the last decades reveals that tectonic boundaries traditionally interpreted as "simple" folded thrusts (e.g., Escher et al., 1988), are actually the complex result of both contractional and extensional tectonic phases (e.g., Ballèvre and Merle, 1993; Wheeler and Butler, 1993; Reddy et al., 2003; Manzotti et al., 2014b). For this reason, most boundaries between tectono-metamorphic units (i.e., discrete crustal elements defined by a peculiar association of lithology, metamorphic imprint and deformative evolution) are not to be named simply as "thrusts" but are more generally referred to as tectonic boundaries (Dal Piaz et al., 2010).

These tectonic boundaries, in their last evolution, represent the most continuous geological discontinuities in the area, while smaller scale lithological contacts are strongly stretched and folded and more discontinuous. The tectonic boundaries are also the best markers between the contrasting metamorphic or chronologic domains, and to evidence the effect of two sets of post-metamorphic brittle normal faults that affect the area at all scales (Bistacchi and Massironi, 2000; Bistacchi et al., 2000, 2001; Sue et al., 2007).

In the following sections we introduce the tectonic architecture of the studied transect. We refer to the tectonic map (Fig. 1) and to the tectono-metamorphic legend (Fig. 2) to unfold the relative positions between tectonic structures. For more detailed descriptions on the tectonic and metamorphic evolution of the introduced units, we refer the reader to the cited literature.

2.1. The Western Austroalpine nappe system

The structurally highest tectonic element of the Northern Aosta Valley is represented by the collisional Adriatic nappe stack, showing eclogitic or blueschist peak metamorphism and greenschist facies regional overprint (Frey et al., 1974; Compagnoni et al., 1977; Compagnoni, 2003). The highest structural position is occupied by the Adriatic Dent Blanche-Sesia Lanzo system (Argand, 1909, 1911; Manzotti et al., 2014b, 2014a). The Dent Blanche system, usually referred to as Argand's Dent Blanche nappe s.l., comprises two different basement sub-nappes, the capping Dent Blanche s.s. and the underlying Mont Mary-Cervino superunit. The former is composed of the kinzigitic Valpelline unit and of the metamorphic Permian granitoids and mafic intrusives of the Arolla unit (Argand, 1906; Dal Piaz, 1999; Manzotti et al., 2014a; Dal Piaz et al., 2016). It is separated from the lower Mt Mary-Cervino Upper and Lower units (Reddy et al., 2003; Dal Piaz et al., 2016) by the Roisan Cignana Shear Zone (Canepa et al., 1990; Manzotti et al., 2014b; Dal Piaz et al., 2016). This shear zone is defined by high strain slices of Mesozoic meta-sediments and pre-Alpine continental rocks. Moving to the internal (Eastern) side, the Adria-derived Austroalpine continental units are represented by the Pillonet klippe (Dal Piaz and Sacchi, 1969; Dal Piaz, 1976; Cortiana et al., 1998) and by the Sesia-Lanzo zone (Compagnoni et al., 1977; Lardeaux and Spalla, 1991), including in the

transect considered here only the frontal Gneiss Minuti Complex. Other continental slices interpreted as Adria-derived extensional allochthons are tectonically interleaved within the ophiolitic units, and are collectively indicated as Austroalpine inliers (Dal Piaz, 1999; Dal Piaz et al., 2001, 2016).

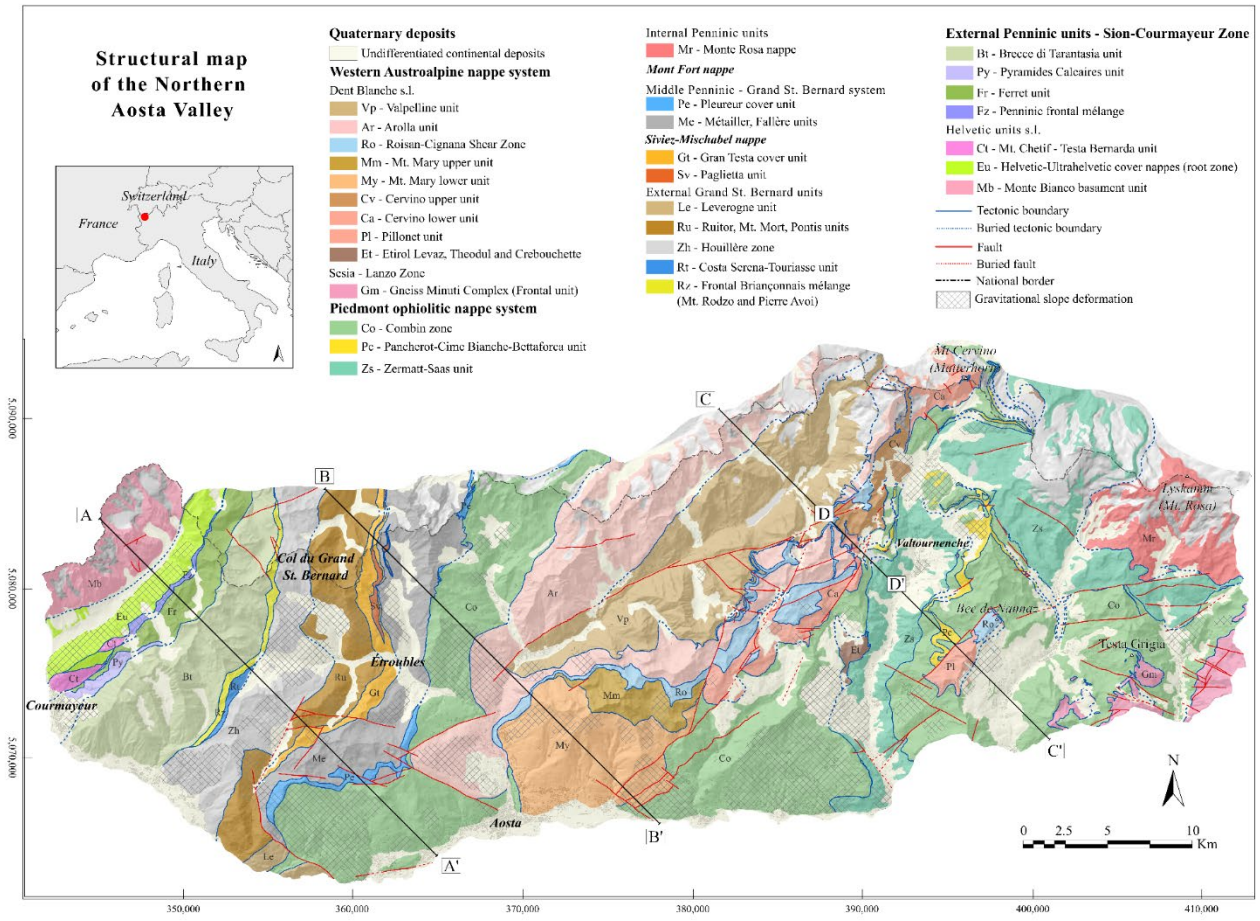

Figure 1. Tectonic map of the Northern Aosta Valley, from Geoportale Regione Valle d'Aosta (https://geoportale.regione.vda.it/). The coordinates at the edge of the maps are provided as WGS 1984, UTM Zone 32.

2.2. The Piedmont ophiolitic nappe system

The Dent Blanche-Sesia Lanzo system overrides the Piedmont ophiolitic nappe system, Argand's (1916) *géosynclinal piémontais*, which in turn is composed by the Combin and Zermatt-Saas zones (Dal Piaz, 1965; Bearth, 1967; Caby, 1981). An interlayered corridor of continental carbonatic and silicoclastic sediments (Pancherot-Cime Bianche-Bettaforca unit; Dal Piaz et al., 2016) is found along or close to the basal contact of the Combin zone, overlying in the second case a lower Combin unit. The Combin and Zermatt-Saas ophiolitic units, separated by the Combin Fault tectonic contact (Ballèvre and Merle, 1993), show contrasting lithology and metamorphic history. Blueschist facies relics register peak metamorphic conditions for the Combin zone (Caby, 1981; Manzotti et al., 2021), while eclogitic and locally (ultra-) high pressure metamorphism (Ernst and Dal Piaz, 1978; Reinecke, 1991; Frezzotti et al., 2014) are recognised in the Zermatt-Saas unit.

2.3. The Penninic continental nappe system

In the North-Eastern portion of the study transect, the ophiolitic Zermatt-Saas unit lies over the eclogitic Monte Rosa continental nappe, derived from the European passive margin (Dal Piaz, 1999, 2001, 2004; Lapen et al., 2007; Steck et al., 2015).

Moving towards the Western and structurally lower units, an intermediate sector is represented by the Grand Saint Bernard nappe system, a thick imbrication of thrust sheets characterised by alpine blueschist to greenschist facies metamorphism (Caby, 1968; Escher et al., 1988; Gouffon, 1993; Sartori et al., 2006; Bergomi et al., 2017). Within this system, the structurally highest and internal unit is the composite Mont Fort nappe (Gouffon, 1993; Burri et al., 1998; Pantet et al., 2020). This nappe is composed of polymetamorphic basement units and associated cover metasediments (e.g., Pleureur unit; Burri et al., 1998) and it is in contact with the overlying Combin zone through the previously mentioned Combin Fault (Ballèvre and Manzotti, 2019). In a more external and lower structural position we find the Siviez-Mischabel and Ruitor units (Caby, 1968; Burri, 1983; Gouffon, 1993; Malusà et al., 2005). Finally, the Houillère zone (Bigi et al., 1990; Bertrand et al., 1996) and the Costa Serena-Touriasse units define the lowermost element of the Grand Saint Bernard nappe system.

The External Penninic units, or Sion-Courmayeur zone (Trümpy, 1954; Elter, 1960), constitute the most external portion of the Penninic nappe system and lie in the Western region of the study transect. Here the peak metamorphism is low-T greenschist facies, with the exception of the Versoyen area which is affected by HP metamorphism. A sequence of younger thrusts defines an imbrication of thrust sheets of decolled cover units and thin basement slices (Dal Piaz et al., 2003). The External Penninic units are represented by the Brecce di Tarantasia unit (Trümpy, 1952, 1955; Elter and Elter, 1965; Loprieno et al., 2011), the Ferret unit (Cita, 1953; Burri and Marro, 1993), the Pyramides Calcaires unit (Antoine, 1971) and the Penninic frontal slices (cataclastic rocks marking to the Penninic Frontal thrust).

2.4. The Helvetic and Ultrahelvetic units

The External Penninic units are in contact, through the Penninic Frontal thrust (Ceriani et al., 2001; Perello et al., 2011), with the "root" of the underlying Helvetic and Ultrahelvetic units (Baretti, 1881; Cita, 1953; Elter, 1960) composed of shallower basement slices and décollement cover units. In the lowermost structural position exposed at the head of the Aosta Valley, we find the basement of the Monte Bianco (von Raumer and Bussy, 2004).

3. The geomodelling workflow

The complex tectono-metamorphic setting of the North-Western Alps and the nature of the input database composed of field data only (i.e., geological and structural data collected at surface) motivate the following geomodelling workflow. Spatial orientation analysis of geological and structural data is followed by structural interpretation on a series of vertical cross-sections, where interpretative models and prior knowledge gained from structural analysis are applied. Eventually, field data and cross-section interpretation are used as input for implicit interpolation, producing three-dimensional surfaces that represent boundaries of tectonic units interrupted by brittle fault surfaces. At each step, particular care is taken to reduce subjectiveness as much as possible. The following sections address in detail each step of the geomodelling workflow, schematically illustrated in Fig. 3.

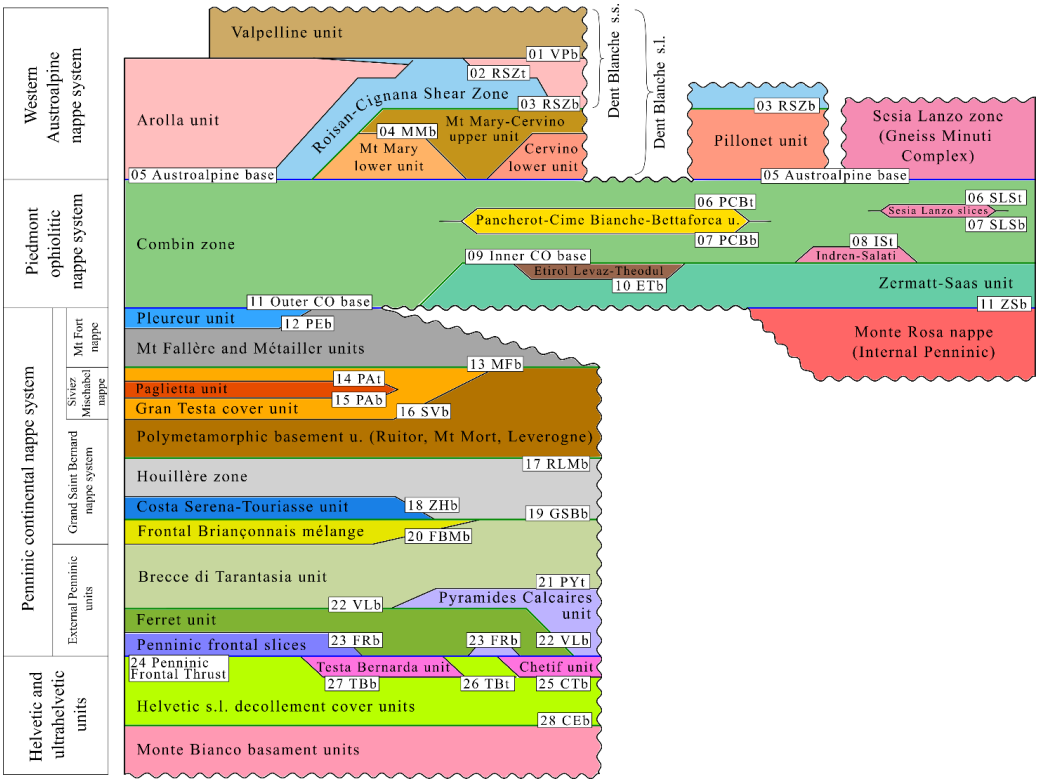

Figure 2. Hierarchical scheme of the tectono-metamorphic relationships of the nappe stack in the Northern Aosta Valley. Major Alpine tectonic contacts separate different nappe systems (i.e., Austroalpine, Piedmont, Penninic and Helvetic and Ultrahelvetic nappe systems) and hold the highest hierarchical importance. Lower hierarchical positions are reserved for tectonic contacts that might interrupt against higher order elements and create tapered geometries. We refer to the text for the detailed description of the tectono-metamorphic legend and to Fig. 1 for the tectonic map.

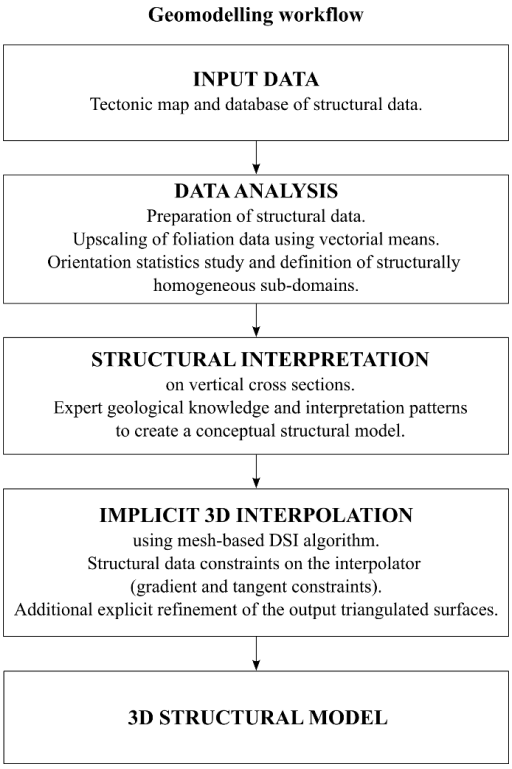

Figure 3. 3D geomodelling workflow. The input tectonic map collects geological information and structural measurements. Structural data (foliation and fold axis measurements) are analysed through an orientation statistics study and foliation data are upscaled to fit the regional extents of the area. Structural interpretations on a network of vertical cross-sections make up the conceptual model. Finally, the implicit DSI algorithm is applied to create the 3D structural model. Detailed description of the workflow in Sect. 3 of the text.

3.1. Input data

Input data for geomodelling projects can be of diverse nature including fieldwork observations, geophysical datasets, well logs, topography (i.e., Digital Elevation Models, DEM) and remote sensing (aerial or satellite) imagery. In our case subsurface data (wells and geophysics) are not available. The Northern Aosta Valley is not crossed by any deep crustal seismic line, with the closest being the CROP-ECORS (e.g., Nicolas et al., 1990) and the NFP-20 (e.g., Pfiffner et al., 1997). The lack of subsurface data is partly counterbalanced by the rugged topography of this sector of the Alps, characterised by a difference in elevation of ca. 4,300 m (from ca. 500 m near Chatillon to 4,809 m on top of Mont Blanc), and by large mountain faces with continuous outcrops.

Our input field data are thus the collection of all the geological, petrographic and structural observations that have been gathered in the field, and of remote sensing and topographic datasets. The project benefits from a recent and homogeneous seamless 1:10,000 geological map (Dal Piaz et al., 2010, 2015; Perello et al., 2011; Polino et al., 2015; and Monte Bianco and Gran San Bernardo sheets under way) which has been synthesized in 1:150,000 and 1:100,000 geotectonic maps of the Aosta Valley (Giusti et al., 2003; Bonetto et al., 2010) and more recently in a 1:75,000 structural map covering ca. 1,500 km^2 (Fig. 1). The dataset is strongly interdisciplinary and, for instance, dense meso-structural observations collected on outcrops (attitude of bedding, foliations, lineations, fold axes and axial surfaces, fractures, faults, etc.) are complemented by petrographic and microstructural studies that help building a consistent structural framework, with different deformation events arranged in a consistent relative chronology. Remote sensing datasets are represented by a 2 m resolution DEM, obtained from a LIDAR survey, and 20 cm/pixel aerial orthophotos (provided by the Autonomous Aosta Valley Region). All these data are organised in a Geographic Information System (GIS) aimed at structural analysis.

3.2. Defining the tectono-metamorphic legend

As in a geological map, the legend of a 3D geomodel is essential to list all the structural and geological features that are represented in the model and define their structural and chronological relationships (including primary and secondary stratigraphic, intrusive and deformation structures). Moreover, the legend defines a unique name for each structural element, which can be used for display, spatial queries and interoperability purposes.

As opposed to the case of sedimentary settings in which the legend is typically represented in the form of a stratigraphic column, sometimes including unconformities as the only complexity (Mallet, 2004), polydeformed metamorphic orogenic settings require a different approach to represent their structure and define the tectonic evolution. In this work we define the tectono-metamorphic legend of Fig. 2 as the 2D schematization of complexly deformed 3D tectono-metamorphic units, intended as discrete elements with a specific metamorphic and lithological history separated by tectonic boundaries.

Tectonic boundaries are represented in the tectono-metamorphic legend as hierarchical lines. First order elements hold the higher importance and, in our model area, do not interrupt against other structures. These are usually major discontinuities that accommodate large displacements (e.g., Austroalpine, Piedmont and Penninic base in Fig. 2). Lower order lines may interrupt against higher order ones, defining lenses and tapered geometries, and they might represent either (i) structures of lower tectonic importance, or (ii) older discontinuities that have been cut by more recent ones (e.g., the Roisan Cignana Shear Zone separating the Dent Blanche s.s. units from the Mont Mary units).

3.3. Structural data analysis

Structural data consist of orientation data of compositional layering, schistosities and mineral lineations (related to different tectonic phases and PT conditions), fold and crenulation axes and axial surfaces of different folding events, and brittle fractures and fault surfaces. Analysis and processing of these data was performed with two goals: (i) defining structurally homogeneous domains, where well-defined interpretation rules could apply, and (ii) interpolating smooth orientation fields that can be used for modelling at the regional scale.

The analysis aimed at defining structurally homogeneous domains (i.e., areas characterised by foliation with constant mean attitude and/or folded along the same mean fold axis) has been performed by applying spherical statistics to data. In stereogram views for data visualisation, mean vectors (Borradaile, 2003) have been computed on populations of fold axis and foliation data (on the normal vectors to the foliation plane). Tentatively, homogeneous domains have been defined with the same boundaries as tectono-metamorphic units, then adjoining domains showing the same statistics have been merged (independently from isotopic ages and PT conditions). Conversely, when some domain revealed a relevant inhomogeneity (i.e., multimodal distribution of foliation data or fold axes), it has been split in two or more parts. The result of this analysis (Fig. 4A) is that each domain is either dominated by folding (hence characterized by average fold axes and/or axial surfaces), or by quasi-planar foliation (this could be either due to very intense lamination, or to almost no deformation).

Smoothing of structural data at the regional scale was performed by averaging orientation data at the nodes of a 650 m by 500 m regular grid (Fig. 4B). The calculation of the vector mean was performed as in Vollmer (1995) and in Carmichael and Ailleres (2016). We excluded structural measurements located within the regions identified as gravitational slope deformation in the map (Fig. 1) from the entire structural analysis. These areas are affected by Deep-Seated Gravitational Slope Deformations, large slow slope instabilities commonly found in mountainous environments which might cause rotation and tilting of data, making them unreliable for the structural analysis.

Structural data analysis led to identifying three macro-regions that can be considered homogeneous in terms of regional-scale orientation statistics, and ductile and brittle deformation styles. The first area corresponds to the most internal sector, where the collisional wedge presents units with high-pressure metamorphism (the Penninic Monte Rosa, the Piedmont Zermatt-Saas unit and the Etirol-Levaz and Theodul lower eclogitic outliers) paired with structurally adjacent greenschist-facies units with blueschist relics (the Dent Blanche-frontal Sesia Lanzo system and the Combin unit). The Inner Combin base (Combin Fault in Ballèvre and Merle, 1993) is responsible for the relative juxtaposition of the blueschist-greenschist units on top of the eclogitic units, showing a planar geometry that sharply cuts poly-folded older lithological and tectonic boundaries. This sector was also heavily affected by brittle post-nappe deformation, as two sets of normal faults offset the tectonic boundaries (NE-SW striking and NW-SE striking; Bistacchi and Massironi, 2000).

Moving towards the external sector, a change in deformation style is registered. The Grand Saint Bernard system (Mont Fort nappe, Siviez-Mischabel nappe, Ruitor and Houillère units) is affected by backfolding in the style of the famous Siviez-Mischabel structure (Milnes et al., 1981; Cartwright and Barnicoat, 2002) involving both basement and cover units. Post-nappe brittle deformation also affected this area, but in a less penetrative way and NW-SE striking normal faults dominate.

Lastly, the external Penninic units and the Helvetic system define a sequence of sub-parallel thrust sheets with thin interposed slices and extensional-transtensional features along more important tectonic boundaries (the Penninic and Briançonnais frontal thrusts). Tectonic boundaries dip with an intermediate angle towards the SE. Moreover, in this sector almost no post-nappe brittle deformation has been mapped that is relevant at the scale of the 3D model. However, the difference in abundance and pervasiveness of large-scale brittle structures may be apparent, as related to the different

competence of outcropping lithologies. In fact, this sector is dominated by soft lithologies (i.e., metasediments), in contrast with the crystalline basements of the collisional wedge, and fault structures might be masked by detrital covers.

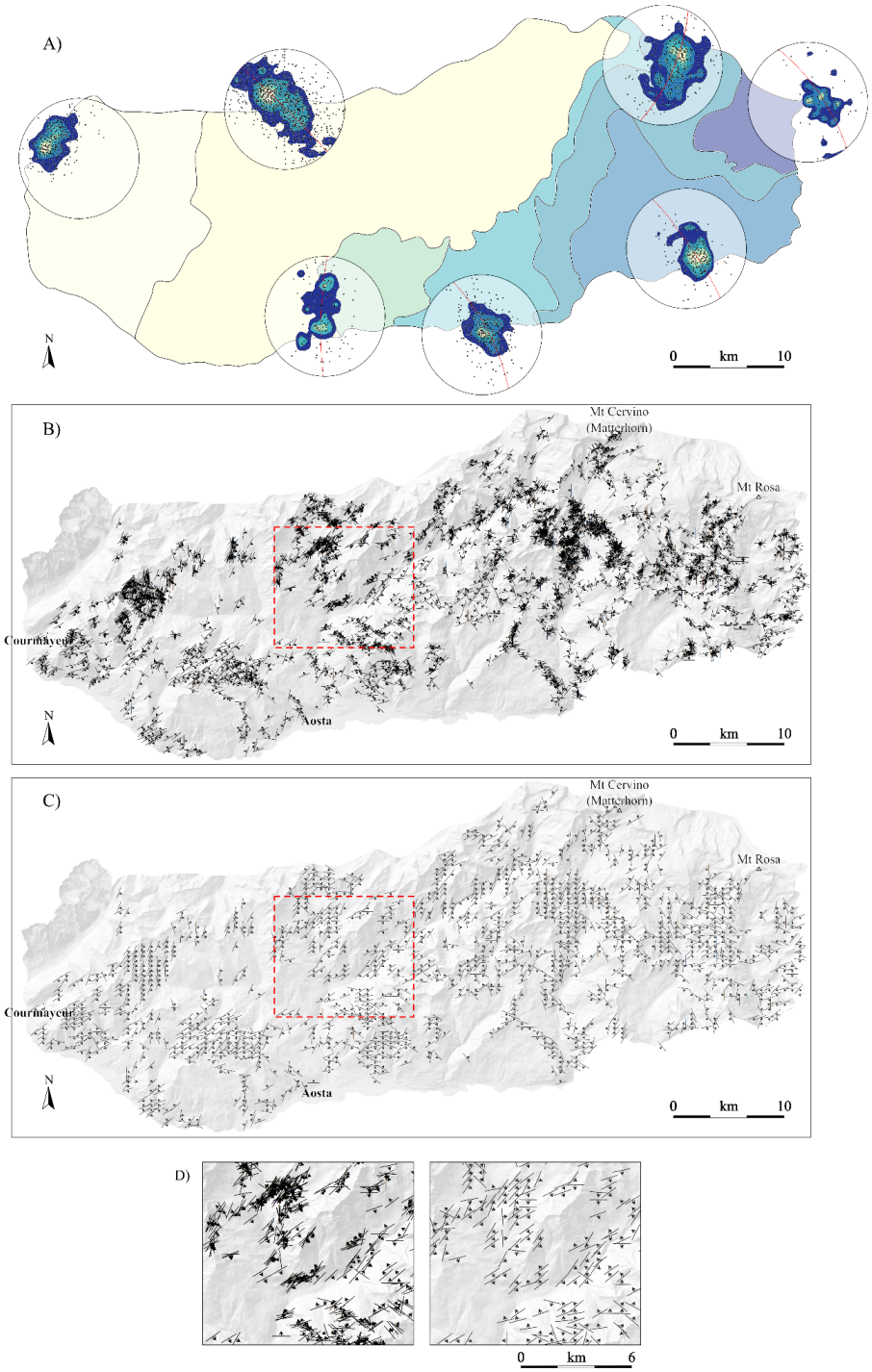

Figure 4: Structural analysis of the Northern Aosta Valley, limited inside the national border to the North and to the Dora river to the South. (A) Homogeneous structural domains. Normal to foliation planes are plotted as dots in stereograms, including contouring with interval 1%. Best fitting as red great circles. (B) Primary foliation measurements at the location of observation. (C) Foliation orientations from B averaged on a 650 m by 500 m regular grid. (D) Details from B and C, from the areas highlighted by the dashed red rectangles.

3.4. Structural interpretation

Deformation structures in metamorphic terrains are characterised by frequent thickness variations, complex multi-phase and sometimes non-cylindrical folding patterns, and large-scale boudinage (resulting in fragmentation of original lithological or stratigraphic units). The geometry of folds, defined by amplitude, wavelength and curvature parameters, often display multi-scale and disharmonic patterns and is influenced by the rheological characteristics of the rocks they deform. Therefore, a conceptual geological and structural model is needed most of the times to guide the interpolation of a consistent 3D model. In agreement with different authors (Kaufmann and Martin, 2009; Zanchi et al., 2009) we build the conceptual model using serialised vertical cross-sections, whose position, spacing and orientation is chosen according to (i) map and model scale, (ii) the distribution of outcrops, (iii) outcomes of orientation analysis and (iv) typical wavelengths of structures in the study area. In particular, the orientation of cross-sections is chosen perpendicular to fold axes and fault surfaces, so as to minimise distortion due to apparent dip effects. Spacing of cross-sections is chosen to be smaller than the wavelength of the smallest folds or fault blocks to be represented in the model. In our case, we built a network of 75 planar vertical cross-sections with horizontal spacing of ca. 1,500 m and distributed in two perpendicular sets, with SE-NW (135°-315° N) and NE-SW directions (Fig. 5). The network of cross-sections has been built in the software Move™ (www.petex.com/products/move-suite), which implements useful tools for data projection and two-dimensional structural interpretation.

Finally, it is a good practice to locate key cross-sections in areas of strong structural complexity, where data sampling is ideally denser. In such areas, depending on the complexity of the structure, it could be useful to densify the interpretation by building additional intermediate cross-sections. This approach was implemented in three specific subareas of the 3D model for the representation of folds with strong lateral variability (see Sect. 4, the Valpelline base, the Mont Mary tectonic contact exposed in the Cignana Lake area, and the Outer Combin base; see Fig. 2 for the nomenclature of the tectonic contacts). We proceeded by progressively reducing the distance between cross-section planes by a factor of 2 until achieving a satisfactory representation, reaching a final distance between cross-sections of approximately 375 meters (one fourth of the original value) for the three subareas.

Interpretation on cross-sections is constrained by orientation data and traces of tectonic boundaries and faults, that are projected onto each section along the mean fold axis or along the mean strike of schistosity defined for each structurally homogeneous subdomain (see Sect. 3.3 and Bistacchi et al., 2008). Since the homogeneous subdomains cover large areas, local geometries occasionally rotate from the average attitude (e.g., due to local rotation of fold axes). To resolve these instances, we locally revisit the orientation statistics analysis, and projection is performed using locally adapted mean vectors.

As a general rule, the projection of structural data and traces of tectonic or lithological boundaries is performed within a buffer of generally half the horizontal spacing between two cross-sections, so that every object in the input dataset is projected onto one cross-section only. However, the maximum projection distance can be varied also according to higher/lower cylindricity of the data (which can be evaluated in the orientation analysis), data density, etc.

When all constraints have been properly projected (as in the synthetic example in Fig. 6), cross-sections in Fig. 5 are interpreted using classical "manual" digitization of all structures by an expert of regional geology. Sometimes the drawing can be aided by algorithms that allow automatically generating patterns of foliations or folds according to some geometric/structural rule (e.g., parallel vs. kink vs. similar folds).

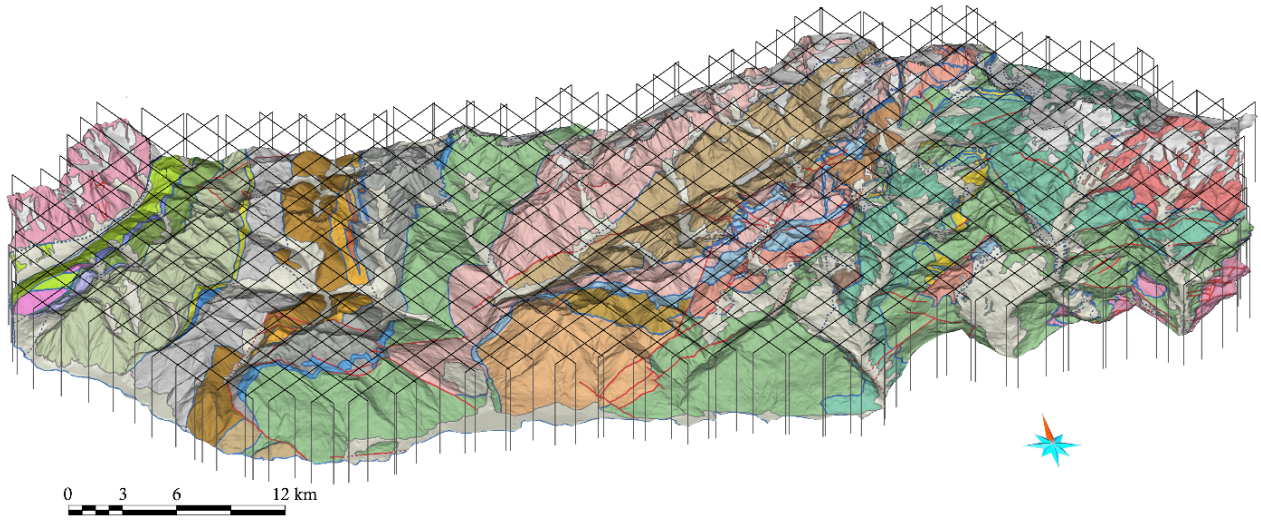

Figure 5. Network of vertical cross-sections on which the conceptual structural model is built, interpreted as detailed in Sect. 3.4 of the text, . The tectonic map (Fig. 1) drapes the topography. Scheme of the tectono-metamorphic relationships in Fig. 2.

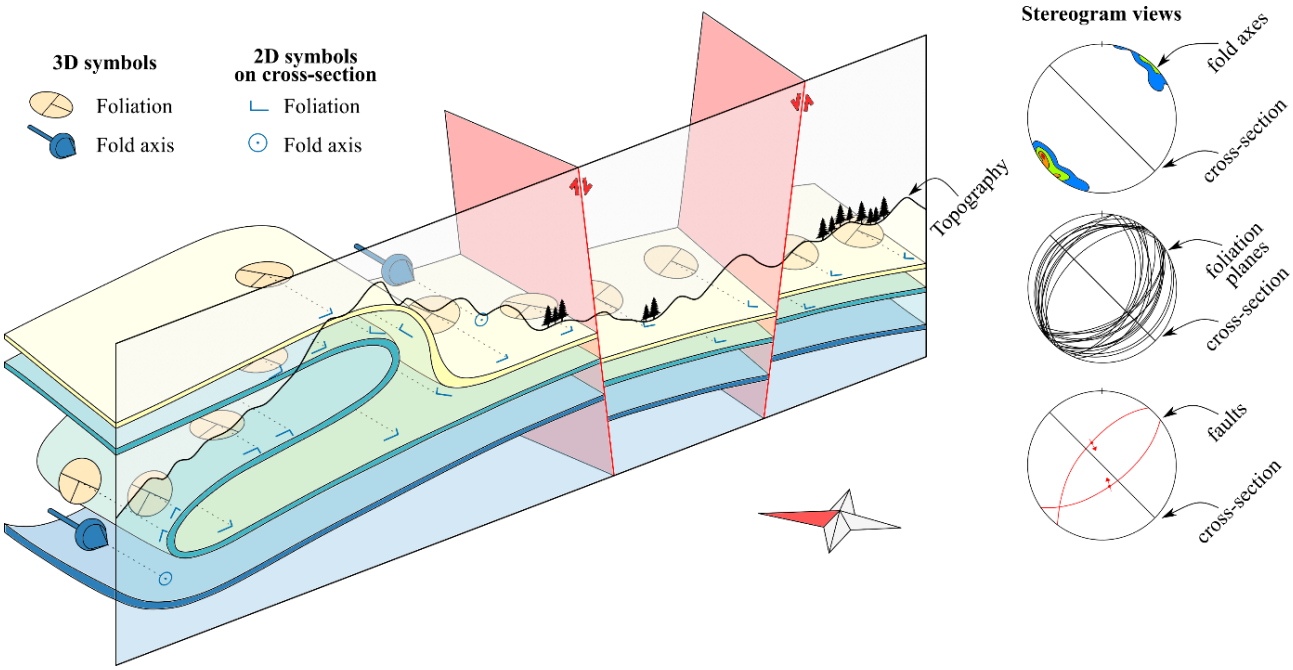

Figure 6. 3D view of a synthetic scenario showing isoclinal recumbent folding and normal faulting. An interpretative cross-section is built by projection of structural and geological data, collected during fieldwork, along the mean fold axis direction.

In our workflow both the subsurface and the eroded space (i.e., below and above the topographic profile) are interpreted. This leads to higher continuity of the interpretation, better expression of structural rules used by the interpreter, better exploitation of rugged topography, and overall higher robustness of the interpretation by avoiding edge effects. Fig. 7 holds examples of cross-sections from our modelled area.

It is well known that building a conceptual structural model is susceptible to subjectiveness of interpretation (e.g., Bond, 2015). However, in our experience this is a lesser evil, necessary to guide the interpolation on the basis of concepts of structural analysis not easily implemented in interpolators used for simple sedimentary sequences with little deformation or very dense sampling interpreted from geophysical images.

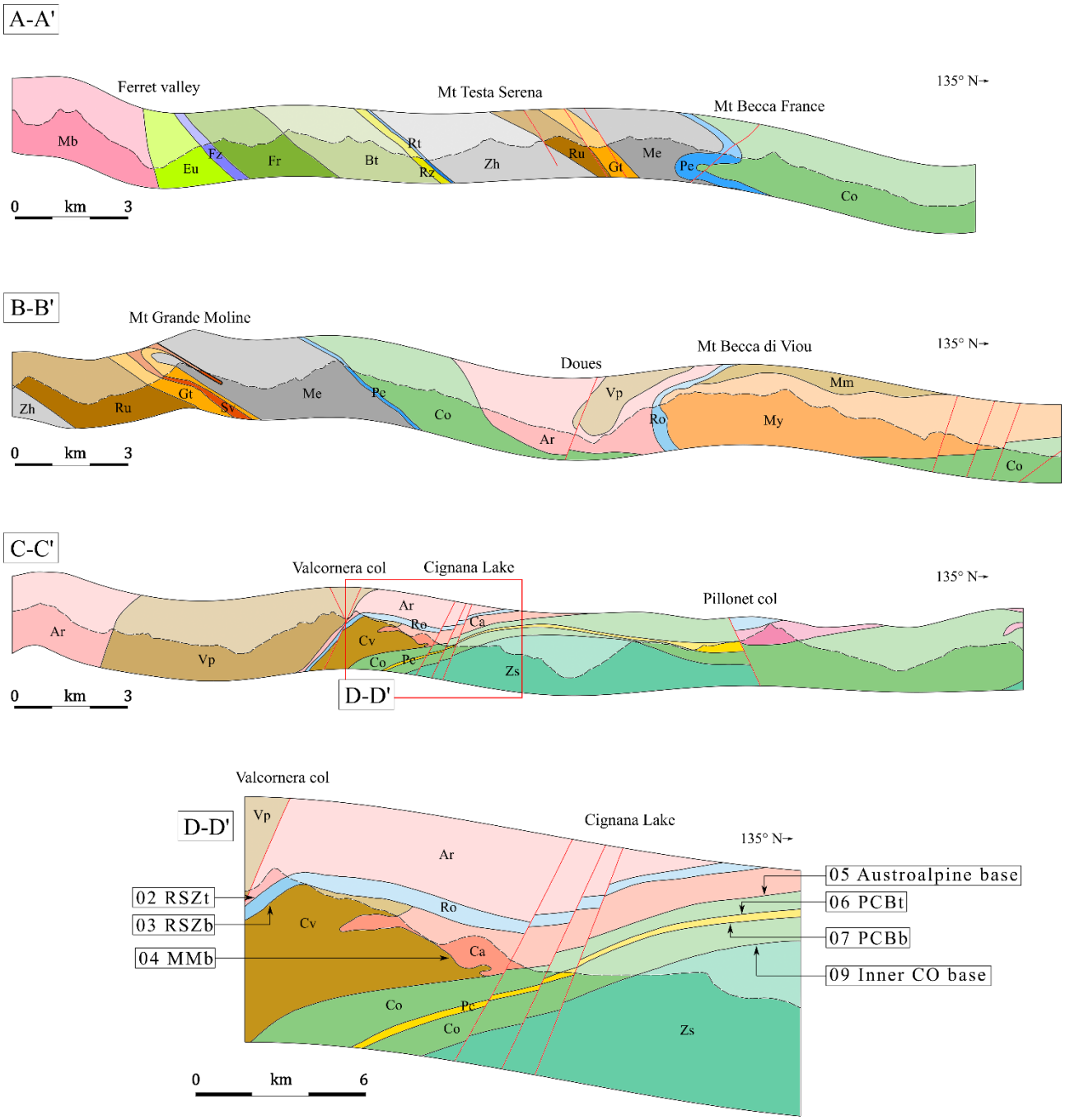

Figure 7. Representative NW-SE cross-sections from the model area. Cross-section locations as in Fig. 1. Colours as in the tectonic legend in Fig. 2. Topographic profiles as dashed black lines.

3.5. Implicit interpolation

We perform the interpolation of implicit surfaces with SKUA/GOCAD® (https://www.aspentech.com/en/products/sse/aspen-skua) and the RING Toolkit plugin, that implement the implicit Discrete Smooth Interpolator (DSI; Frank et al., 2007; Caumon et al., 2013). The interpolation is solved on a tetrahedral mesh using a least-squares weighted approach leveraging different kinds of geological and structural constraints. These are classified as hard (i.e., to be strictly honoured) or soft constraints (i.e., to be honoured in a least-squares sense).

Geological constraints are further distinguished in position and gradient constraints, respectively influencing the value of the scalar field or the orientation of its gradient (Frank et al., 2007; Caumon et al., 2013). Position constraints correspond to mapped tectonic contacts, interpretations on vertical cross-sections or observations along boreholes (not available for our model) and define the value of the scalar field at the corresponding locations. Gradient constraints allow instead the incorporation of structural data (e.g., foliation data and fold axes) to constrain the orientation of the implicit surfaces to conform to structural trends (Frank et al., 2007; Caumon et al., 2013).

Constraints obtained from the previous steps of our workflow are assigned different weights, or certainty levels, with the higher value corresponding to direct field observations such as outcropping tectonic boundaries and structural data. Meanwhile, conceptual interpretations in vertical cross-sections are assigned a lower weight/certainty level since they result from expert geological interpretation and can be at least partly imprecise or subjective. An additional constant gradient constraint is used to guarantee continuity across cells of the tetrahedral mesh and hence the well-posedness of the mathematical interpolation problem (Frank et al., 2007; Caumon et al., 2013). This constraint is generally isotropic and constant throughout the entire model volume, however the *Structure and Stratigraphy* workflow of SKUA/GOCAD® enables, if requested, variations in the magnitude of the gradient of the scalar field, allowing large thickness lateral variabilities to be modelled.

Faults are introduced in the model in an early step, in the form of explicit triangulated surfaces, interpreted from their mapped trace as it curves along the DEM, and extended up- and down-dip proportionally to their map length. Cross-cutting relationships amongst fault surfaces are based on map relationships and relative chronology. Since fault surfaces interrupt the continuity of the implicit scalar field, they are introduced in SKUA/GOCAD® as internal boundaries in the tetrahedral mesh, with tetrahedra being disconnected on opposite sides of a fault, resulting in mathematical discontinuities in the interpolated scalar field. This modelling strategy allows to introduce in the model both faults cutting through the whole domain and finite faults having tip lines inside the modelled volume (Frank et al., 2007; Caumon et al., 2013).

In Fig. 8 we schematically show the result of the implicit interpolation, which leverages the classes of constraints introduced before, on the synthetic scenario already presented in Fig. 6. This picture represents the implicit scalar field interpolated on a tetrahedral mesh in a three-dimensional volume, and surfaces of interest extracted a posteriori as isovalue nodes. The scalar field is interrupted by two normal faults, which dissect the conformable mesh. Foliation and fold axes are imposed as gradient constraints on the scalar field, allowing to easily model the isoclinal recumbent fold.

Due to the variability in deformation mechanisms and structural style, for the interpolation of our regional-scale 3D model we exploit the *divide et impera* principle. The whole area is subdivided into sub-models defined on similarity of deformation styles (i.e., the three macro-regions defined in Sect. 3.3, corresponding to the Austroalpine-Penninic wedge, the Grand Saint Bernard system and the external Penninic and Helvetic units), and the interpolation is performed in separate steps. This allows different geomodelling solutions to be applied to handle the complexities of the different sub-areas, as explained in the present section.

The tectonic boundaries of units outcropping in the Western portion of the Northern Aosta Valley (i.e., the External Penninic units and the Ultrahelvetic-Helvetic domain, Fig. 2) show in some cases lenticular geometries due to the presence of duplex structures in the stack of thrust sheets (Fig. 1). Some units of the Austroalpine and Piedmont nappe systems (Fig. 2, the Mont Mary tectonic contact, and the Etirol-Levaz and Indren-Salati units) also show lenses with limited areal extent, in this case due to ductile shearing (Fig. 1). In both cases, the geomodelling problem is resolved by interpolating with the *Structure and Stratigraphy* workflow in SKUA/GOCAD®, which implements an implicit interpolator based on the previously mentioned DSI algorithm (Frank et al., 2007; Caumon et al., 2013). This workflow allows the definition of "unconformities" (using a term borrowed from stratigraphy) as interruptions of the continuity of the scalar field, that permit obtaining closed lenticular volumes.

Other portions of our model, such as the Dent Blanche s.l. and the basement units of the Grand Saint Bernard, include tight and isoclinal folds with long limbs and tight hinge zones (Fig. 1), which are better constrained by the RING Toolkit plugin implicit interpolator (Frank et al., 2007; Caumon et al., 2013). This tool allows imposing different kinds of structural constraints on the scalar field, each one based on different input data and with a different weight/certainty level. Fold axes and foliation data are used to constrain the gradient of the scalar field to be perpendicular to, respectively, the fold axis vector and the schistosity plane (Caumon et al., 2013). The definition of these additional structural constraints allows leveraging direct field observations, a better control on the modelled geometries, and lower tendency to create unintended artifacts (e.g., "handles" or "bubbles" in the implicit surfaces) when interpolation is conditioned by conceptual interpretation from vertical cross-sections. This approach leverages input data not considered in the SKUA/GOCAD® *Structure and Stratigraphy* workflow - particularly foliation and fold axes, and results in a successful interpolation of tight isoclinal folds.

Successively, we export the implicit surfaces representing faults and tectonic boundaries, corresponding to isovalues in the scalar field, as triangulated surfaces. These output surfaces, constituting the boundary representation of the 3D model, undergo an enhancement step using the explicit tools of SKUA/GOCAD® (Caumon et al., 2004) aimed at seamlessly merging the independently interpolated portions of the model and resolving local intersections. Specifically, we employ mesh-cutting tools to integrate the portion of the Mont Mary tectonic contact that outcrops in the vicinity of the Cignana Lake which, due to its particular complexity (Fig. 7, section C-C'), was modelled independently from the rest of the tectonic architecture. We also utilise explicit tools to complete the representation of lenses created by regional scale boudinage (see the Pancherot-Cime Bianche-Bettaforca lens and the Sesia-Lanzo slice in Fig. 2) which, unlike the other lenticular geometries previously addressed, do not lie on a hierarchically higher tectonic contact in our model. For their modelling, after employing the *Structure and Stratigraphy* workflow and utilising the "unconformity" setting to create lenticular geometries on one of the two surfaces bounding the body, we apply mesh-cutting tools to terminate the second surface at the intersection location. Finally, we leverage explicit tools to rework the triangulated surfaces and increase the equilaterality of the triangles composing the mesh, thereby improving the quality of the output.

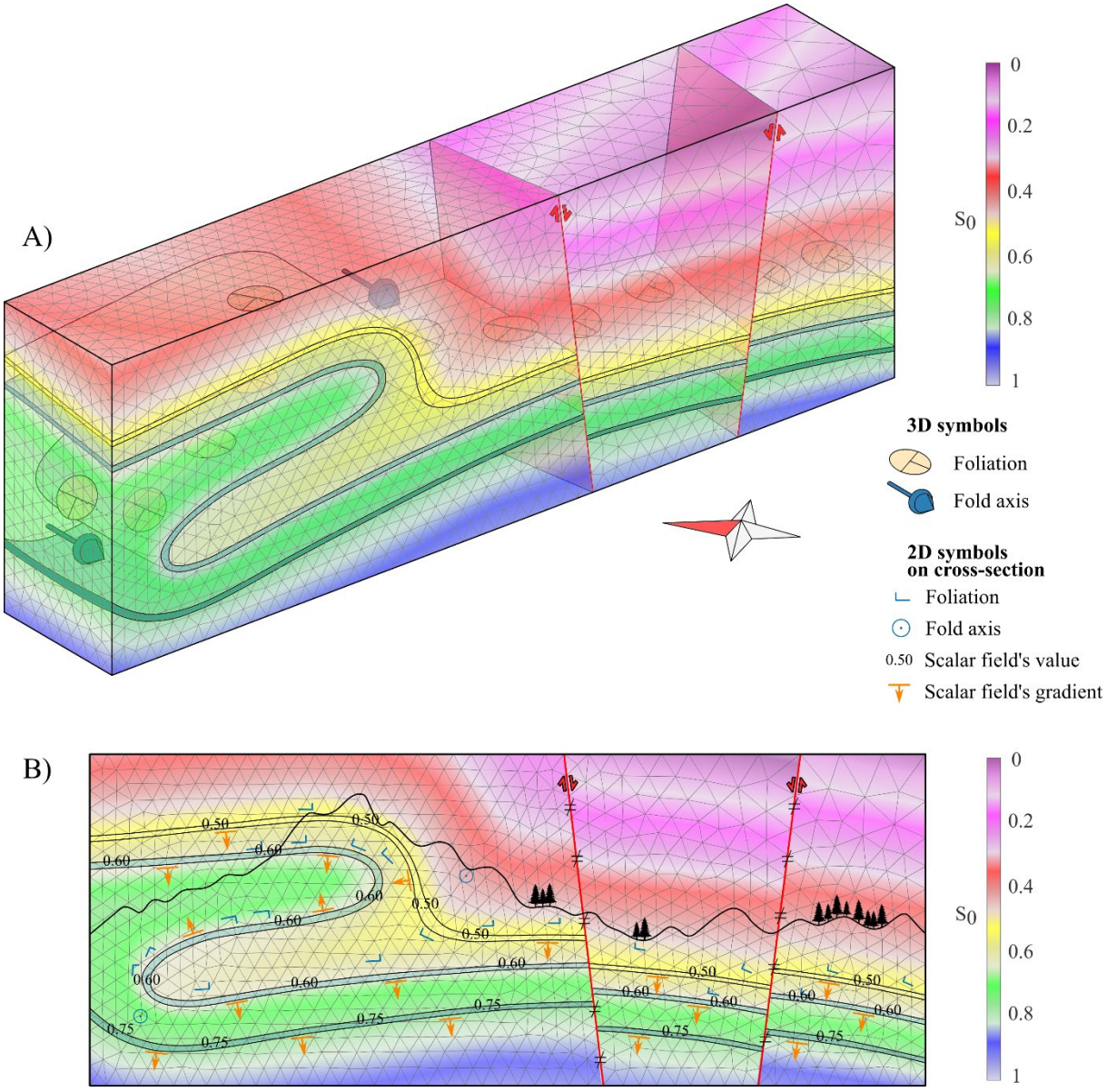

Figure 8. (A) 3D and (B) cross-section views of the synthetic scenario in Fig. 6 displaying isoclinal recumbent folding and normal faulting. The implicit approach is employed to interpolate the 3D structural model, using geological and structural data as value and gradient constraints.

4. The Northern Aosta Valley 3D structural model

The 3D structural model of the Northern Aosta Valley covers an area of ca. 1,500 km^2 and has a vertical extension of ca. 2,000 m, extending above and below the topographic surface. The boundary representation model is displayed in Fig. 9 and 10, and can be interactively explored on https://geologia3d.regione.vda.it.

A total of 29 tectono-metamorphic units is represented in the model, separated by 28 tectonic boundaries which are cut by 81 fault surfaces, all of them with finite surfaces and internal tip lines. The tetrahedral mesh used for the implicit interpolation has a vertical and horizontal resolution of 145 m (corresponding to the average edge length of the tetrahedra) totalling ca. 1.1 x 10^6 nodes and ca. 6.4 x 10^6 tetrahedra. This resolution allows for practical interpolation times on a desktop computer (between 10 and 30 minutes on average for the interpolation of the scalar field) and is suited for the

representation of the gently deformed tectonic contacts of the external portion of the 3D model and for the complexity of the internal collisional wedge.

The core of the studied transect, represented by the Western Austroalpine nappe system, constitutes one of the most complicated volumes of the 3D structural model. The region is characterised by frequent open and isoclinal folded geometries, whose continuity is interrupted by multiple internal hierarchical relationships and a network of brittle normal faults. The major tectonic contact internal to this system is the Roisan-Cignana Shear Zone (Manzotti et al., 2014a). Represented in our model by its bounding top and base surfaces, the Shear Zone is characterised by open undulations at the regional scale and abrupt lateral thickness variations. It closes, to the South, at the intersection with the hierarchically higher Dent Blanche Basal Thrust, whose regional expression is indicated as Austroalpine base in our model to highlight its position in the tectonic sequence (Fig. 2). Overhanging said Shear Zone, only the mylonitic contact between the Valpelline and the Arolla unit outcrops. We represented the Valpelline base surface as a large scale mylonitic isoclinal synform, whose regional fold axes gently plunge towards the NE. The hinge of the regional fold outcrops in the Swiss Alps outside of our model area, North of the Dent d'Hérens-Tête de Valpelline ridge (Dal Piaz et al., 2016).

In underlying position, the tectonic contact internal to the Mont Mary superunit is represented by folded surfaces that interrupt at the intersection with the higher order Roisan-Cignana Shear Zone and Austroalpine base. In the area between the Cignana Lake and the Valconera col (Fig. 7, section CC'), the tectonic contact outcrops as a series of small-scale, isoclinal recumbent folds (Fig. 1). The limited thickness of the fold limbs is sub-scale as compared to the resolution of our 3D model and an accurate representation of the geometry would require a much finer mesh and impractical run-times. In fact, the DSI approach solves linear equations inside each tetrahedra, and higher curvature would be necessary to accommodate the narrow isoclinal geometry. Therefore, in our model this portion of the Mont Mary tectonic contact slightly diverges from the tectonic map and we modelled it as a close recumbent fold. A higher resolution 3D model, focusing on this area, will be addressed in a future publication.

The units outcropping in the vicinity of the Pillonet col are correlated to the Mont Mary superunit and the Roisan-Cignana Shear Zone (Dal Piaz, 1976), although geographically separated by the Valtournenche valley. Therefore, in the 3D model the tectonic boundaries limiting the units in question are modelled as laterally continuous. The Austroalpine nappe system extends towards the East as Sesia Lanzo Zone, which is represented in our model by the Gneiss Minuti Complex only. Its related tectonic slices (i.e., the Sesia Lanzo and Indren-Salati slices, Fig. 2), detached by the main continental body, are modelled as independent slivers geometrically incorporated within the Piedmont ophiolitic sequence.

In lower tectonic positions, we model the Easternmost portion of the Combin Fault (Ballèvre and Merle, 1993) and we refer to it as Inner Combin base (Fig. 2). While the name Combin Fault indicates a major Alpine tectonic contact responsible for the juxtaposition of the Combin zone with the Zermatt-Saas to the East and with the Mont Fort nappe to the West (Ballèvre and Merle, 1993), in our model we refer to the two portions of this tectonic contact using separate names. With this choice we want to highlight the different hierarchical importance that they hold in the tectono-metamorphic legend of our work (Fig. 2).

Incorporated into the ophiolitic Combin zone, we model the Pancherot-Cime Bianche-Bettaforca unit (Fig. 2) as a thin lens that spreads over the Valtournenche and Ayas valleys before laterally closing. Gentle open folds characterise the top and bottom surfaces that define the extents of this tectonic unit. Three additional eclogitic continental lenses, named after close geographical elements, are found along the tectonic limit between the Combin and the Zermatt-Saas units. These are the elements of Etirol-Levaz, Crebuchette and Theodul. Due to coeval ages and conditions of metamorphism (Dal

Piaz et al., 2001), these lenses are modelled to belong to the footwall of the Inner Combin base, together with the Zermatt-Saas unit.

In the North-Eastern sector of the 3D model, the Zermatt-Saas unit overrides the Monte Rosa nappe. As proposed by Lapen et al. (2007), these two eclogitic units show at least partially shared Alpine metamorphic history. Therefore, we model the separating tectonic contact (called Zermatt-Saas base in our model) with open folds geometry, to enhance its reworking under HP metamorphic conditions.

Moving towards Western portions (Fig. 7A), the ophiolitic Combin zone overlies the European Mont Fort nappe along the Western portion of the Combin Fault (named Outer Combin base in our model), defining another first order tectonic limit (Fig. 2). The contact is characterised by tight to isoclinal folds that affect the rocks of the Combin zone and the Mont Fort unit. Their axial plane gently dips towards the South-East and their asymmetry can be interpreted as the result of top-to-SE extensional shear under greenschist-facies conditions (Ballèvre and Manzotti, 2019). Isoclinal folding geometries also affect the contacts of the upper Grand Saint Bernard sequence, the Siviez-Mischabel and Ruitor base. These geometries can be linked to post-nappe reactivation with top-to-SE kinematic. The mathematical problem of modelling these isoclinal folds characterised by thin limbs is the same encountered for the small-scale folds of the Cignana Lake, as discussed before. We thus apply the same geomodelling solution and we model the abovementioned tectonic contacts while maintaining only the geometries that are above the resolution limit of our 3D mesh. The 3D model hence simplifies the folds of the input tectonic map while staying true to the regional folding style.

Finally, a clear change in geometry and metamorphic conditions of the tectonic contacts is registered towards the Westernmost tectonic succession. The thrust sheets of the External Penninic, Helvetic and Ultrahelvetic units constitute the youngest sequence of tectonic contacts and the easiest to model portion of the Northern Aosta Valley. The sequence of thrust sheets shows frequent cross-cutting geometries that add complexity to the modelling and make up the imbricate tectonic structure. We modelled them as quasi-planar tectonic surfaces, parallel to the SE-dipping greenschist facies foliation and affected by gentle folding at the regional scale.

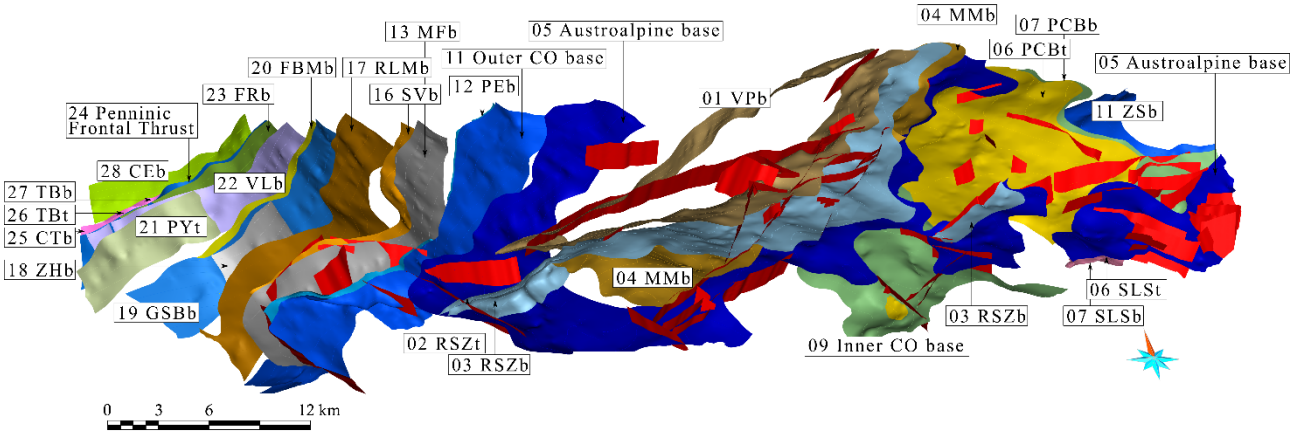

Figure 9. 3D structural model of the Northern Aosta Valley. Tectonic map in Fig. 1 and tectono-metamorphic legend in Fig. 2. Detailed description of model and tectonic contacts in Sect. 4 of the text.

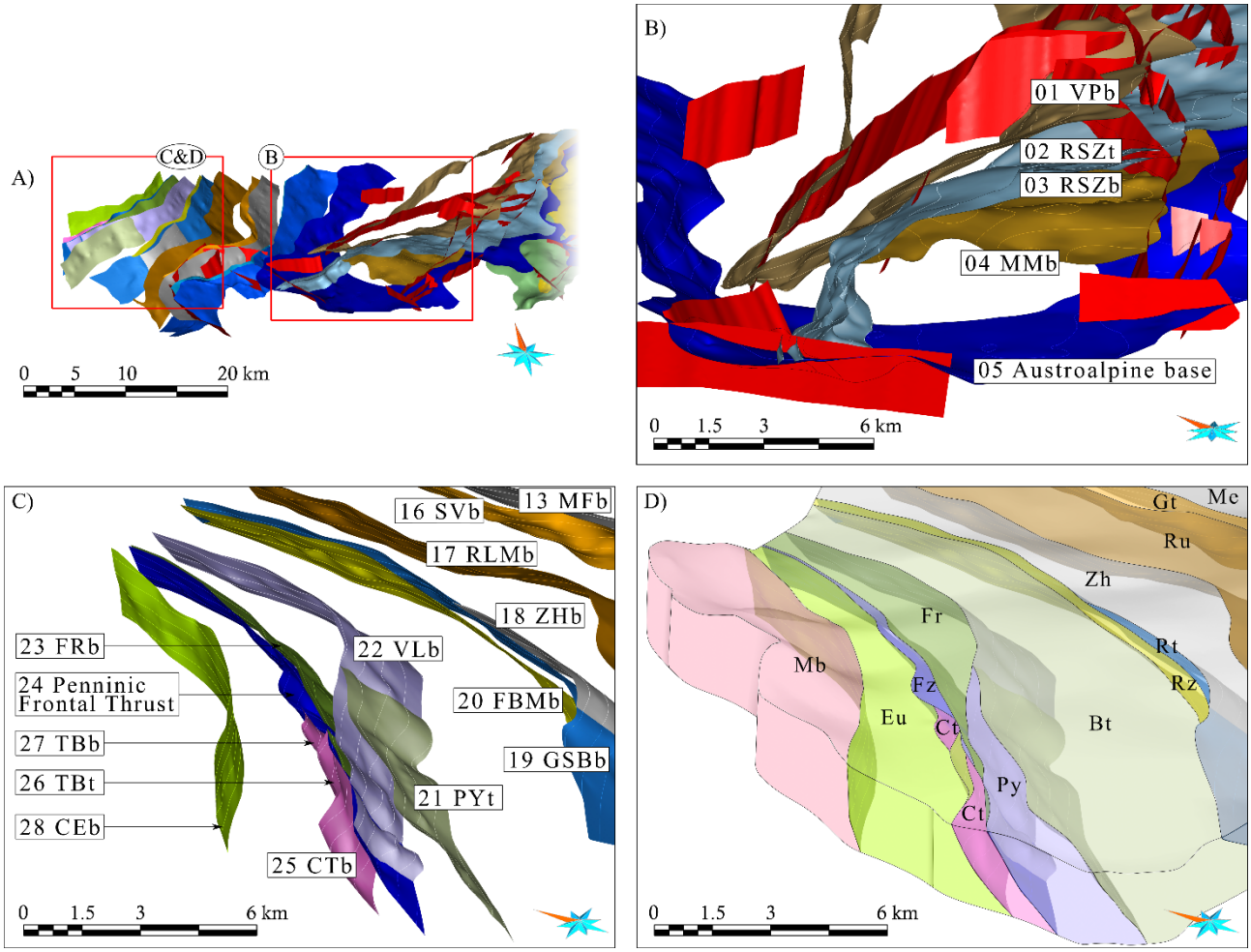

Figure 10. Details of the 3D model in Fig. 9. Tectonic map in Fig. 1, and scheme of the tectono-metamorphic relationships in Fig. 2. (A) Portion of the 3D model with highlighted subareas for (B), (C) and (D). (B) Detail of the boundary representation of the Valpelline base, Roisan-Cignana Shear Zone, Mont Mary tectonic contact and Austroalpine base. (C) Detail of the boundary representation of the Westernmost portion of the 3D model (Penninic and Helvetic nappes). (D) Same subarea as in (C), displaying volumes.

5. Discussion on structural interpretation

The input data of this work is composed of the database of geological, petrographic and structural data collected in GIS and represented in the tectonic map (Fig. 1). Although the difficulties connected to the creation of the tectonic map are not the focus of the present work, we ought to highlight some critical steps in the process. The input map is the result of fieldwork and upscaling from previously published datasets (Geoportale Regione Valle d'Aosta, https://geoportale.regione.vda.it/). The structural model, on the other hand, is the result of the 3D interpolation of a conceptual model created from the knowledge provided by the map and by fieldwork. Although at first sight the workflow appears as a unidirectional process (i.e., the tectonic map affects the 3D model, and not vice versa), the two entities operate a process of mutual validation. For instance, an interpretation that in map view seems correct, might be discussed and improved under the light of three-dimensional reasoning.

This approach has proven instrumental in refining the tectonic map and choosing the best scenario among different interpretative possibilities in the 3D model and in the map. One notable example is provided by the reinterpretation of Gouffon's (1993) *accident col de Bard-Saint Nicolas*, an important

brittle structure exposed in the southern portion of our model, East of Aosta. This fault, which puts in contact outcrops of the Combin zone with units of the Grand Saint Bernard (Fig. 1), was originally interpreted with reverse kinematics (Gouffon, 1993) and is instead represented in our model as a normal fault whose extension towards the South might connect to the Aosta-Ranzola fault (Bistacchi et al., 2001), outside of our 3D model, with abutting relationship. The interpretation of this fault has always been problematic due to the scarcity of available outcrops and due to its NW-SE orientation, which is sub-parallel to the interpretative profiles that are usually drawn to represent the SE-dipping nappe stack. Such sub-orthogonal structures are extremely challenging to interpret using only two-dimensional sections. Three-dimensional reasoning additionally played a crucial role in the final interpretation of the southern portion of the Outer Combin and Pleureur tectonic contacts, exposed South of Étroubles. By combining the structural database displaying sub-horizontal, NE-SW trending fold axes with the 3D topography draped with the map, the presence of large-scale recumbent folds affecting the tectonic contacts became evident and was accurately represented in both the map and the 3D structural model.

To work efficiently, this iterative process of mutual improvement between 2D and 3D interpretation requires the map and the 3D model to smoothly communicate and is the motivation for the definition of the tectono-metamorphic legend in our workflow. By representing the tectonic contacts with unique names and clarifying their hierarchic relationships, this legend simplifies the exchange of data and interpretations between the map and the 3D model.

A fundamental bridge between the two-dimensional map and the three-dimensional model is also provided by the network of vertical cross-sections. By breaking down the 3D model into a series of smaller 2D problems, interpretation at the regional scale becomes manageable. The major downside of building a network of interpretations in vertical cross-sections is the significant interpretation workload. However, at present this is the only known way of transferring geological knowledge of complex poly-deformed structures to the 3D model at this scale.

Another critical aspect regarding the interpretation in cross-sections is the subjectivity that affects the process and the results. Two expert structural geologists, if given the same dataset, would come up with similar but not identical solutions (Bond, 2015). This is because 3D geomodelling is often an under-constrained problem and interpretations are also based on prior knowledge and structural rules issued after assuming particular deformation mechanisms and chronology. One approach to address the subjectivity issue is envisaging the creation of solutions with multiple, geologically feasible, scenarios. While in this paper we presented a single deterministic model to portray the tectonic architecture of the Northern Aosta Valley, we are working on incorporating multiple solutions into the interpretation of particularly interesting subareas, as will be discussed in a future publication.

Another direction of research that could address these limitations and improve the modelling process, in terms of both efficiency and reproducibility, is the exploration of automatic modelling solutions. While a fully automated workflow for the modelling of regional-scale metamorphic settings is still to be developed, different methodologies for the upscaling of geological information to smooth high-resolution datasets to match the model's scale and eliminate the effects of parasitic deformations have been proposed (e.g., Jessell et al., 2014, 2021). In particular, we integrated in our workflow a decimation methodology aimed at averaging foliation measurements along a regular grid (Carmichael and Ailleres, 2016). Nevertheless, the process of structural interpretation on cross-sections remained necessary to interpret large-scale geometries from small-scale deformations observed in the field and registered in the tectonic map, and to achieve geological realism.

6. Discussion on geomodelling methods

3D modelling of the polydeformed metamorphic units of the North-Western Alps is a challenging task. Nevertheless, by applying a model-driven workflow to leverage a rich geological, petrographic and structural dataset, it was possible to build the new 3D structural model of the Northern Aosta Valley. After building a consistent conceptual model in vertical cross-sections, we exploited implicit interpolation algorithms to model the tectonic contacts outcropping in the area.

In the SKUA/GOCAD® environment, the integration of faults by truncated signed distance fields is particularly efficient and the modelling of gently deformed surfaces is extremely straightforward. Tapered geometries and lenses are well-represented using "unconformity" relationships in the SKUA/GOCAD® *Structure and Stratigraphy* workflow, thanks to the definition of mathematical discontinuities inside the mesh.

However, when it comes to tight and/or recumbent geometries, that are in fact very frequent in the geology of the Northern Aosta Valley even at a bigger scale, the software encounters difficulties. The creation of artifacts (i.e., bubbles in the surfaces or a poor fitting of the input data) is likely to happen when the spacing between data and/or the mesh resolution is of the same order of magnitude as the wavelength of the structures. The RING Toolkit interpolator (Frank et al., 2007; Caumon et al., 2013) solves the majority of these problems by defining specific structural constraints for the interpolation. Fold axes and foliation planes guide the implicit scalar field while quantitively honouring a class of input data that holds relatively low uncertainty. The interpolator also allows for fine tuning of the relative weights between constraints in order to better account for direct field measurements vs. more uncertain structural interpretation in cross-sections.

For the modelling of large areas characterised by different deformation styles (e.g., a collisional orogenic wedge paired with a thrust sequence of semi-parallel structures as in our tectonic setting), we advise the subdivision of the model area into smaller sub-areas, where possible, to break down the interpolation of the scalar field in more manageable sectors with relatively stationary structural features.

The resolution of the mesh also has a large impact on the quality of the output, and it must be chosen in accordance with input data density, scale of the geometries to be represented and computational capacity of the machine. At the price of an increased computational cost, a finer mesh allows a more consistent representation of the geometries represented in vertical cross-section and permits smaller scale geometries to be modelled. In this project, we started by building a 3D mesh with low resolution and downsampled by a factor 2 in both vertical and horizontal directions to obtain a high quality mesh manageable by our workstation (AMD Ryzen 9 5950X Processor, 64.0 GB RAM on a Windows system) that would adequately represent the geological complexity of the Northern Aosta Valley. Automatic local mesh refinement (e.g., Frank et al., 2007) could possibly be envisioned in the future to help these aspects.

Relying on structural interpretations on cross-sections for the representation of folds translates into significant subjectivity of the modelling outcome. Previous works proposed the integration of fold axes, fold axial surfaces and overprinting relationships for the modelling of folds (Maxelon et al., 2009; Laurent et al., 2016; Grose et al., 2021). While these approaches could enhance the modelling of the tectonic contacts exposed in our study area, they might not be sufficient for dealing with disharmonic and multi-scale folding, and we envision their application to subareas where more stationary patterns are exposed. Modelling efforts located in the Cignana Lake area are focused on this aspect, as will be discussed in a future publication.

Overall, this study shows that building a large-scale geological model from field data in a region of significant structural complexity remains far from full automation and still calls for significant

modelling skills. In the proposed workflow, significant time was spent to interpret cross-sections, analyse and interpret the field data, experiment with the modelling parameters, the type of information to use and the 3D visualisation until an acceptable 3D geometry was obtained. This process can be seen as frustrating and found inefficient as compared to a (yet-to-be-found) fully automated solution. Nonetheless, even if new and welcome ways to translate geological knowledge into quantitative spatial prediction methods are to be found in the future, and if the level of automation increases in future geomodelling workflows, geological reasoning (*sensu* Frodeman, 1995) will remain fundamental to judge on the geological realism of the results.

7. Conclusions

We presented the new 3D structural model of the Northern Aosta Valley, built with a model-driven implicit modelling approach. Starting from a newly published 1:75.000 geological map and high resolution field structural data only, we built the conceptual model on vertical cross-sections integrating expert geological knowledge. The interpretation is performed following classic geological concepts and structural data projection techniques. The implicit interpolation of the model is performed in SKUA/GOCAD®, that implements both the Discrete Smooth Interpolator and the RING Toolkit interpolator. Together, the two interpolators allow the creation of the challenging geometries that outcrop in the Northern Aosta Valley such as hierarchical shear zones, recumbent isoclinal folds, tapered and lenticular geometries and a network of finite brittle faults whose surfaces and tip lines are internal to the 3D volume.

8. Author contributions

AB conceived and supervised the project. DB acquired funding. AB, BM, GA and GDP carried out fieldwork in the study area and contributed to the tectonic legend, that was originally conceived by AB. BM and GDP managed the GIS and created the tectonic map of the study area (that will be submitted in an independent contribution), with inputs and discussion with AB. GA performed the structural data analysis, with inputs from AB and BM. AB and GA performed the structural interpretation in vertical cross-section, with feedbacks from BM and GDP. GA created the 3D structural model, with feedbacks and guidance by AB and GC. GA redacted the manuscript with inputs and contributions from AB and GC.

9. Acknowledgements

AspenTech is acknowledged for licenses of the SKUA/GOCAD® software. We acknowledge Petroleum Experts (Petex) for providing academic licences of Move™. Our study was supported by the Italy-Swiss Interreg RESERVAQUA project (ID 551749). G. Arienti acknowledges support from the European Union's Erasmus Traineeship + program. We thank G.V. Dal Piaz for personal reviews and comments and for his unvaluable work on the tectonic map of the Northern Aosta Valley that is the synthesis of almost 70 years of fieldwork and detailed analysis.

10. References

Antoine, P., 1971. La zone des brèches de Tarentaise entre Bourg-Saint-Maurice (vallée de l'Isère) et la frontière italo-suisse. Stratigraphie, Université de Grenoble 367 pp.

Argand, E., 1916. Sur l'arc des Alpes Occidentales. Eclogae Geologicae Helvetiae 14, 145–191.

Argand, E., 1911. Les nappes de recouvrement des Alpes pennines et leurs prolongements structuraux. Matériaux Pour La Carte Géologique de La Suisse 31, 1–26.

Argand, E., 1909. L'exploration géologique des Alpes pennines centrales. Bulletin de La Société Vaudoise Des Sciences Naturelles 45, 217–276.

Argand, E., 1906. Sur la tectonique du Massif de la Dent Blanche. Comptes Rendus de l'Académie

Des Sciences Paris.

Ballèvre, M., Manzotti, P., 2019. Ductile shearing on top of the Eocene extruding wedge: the Combin Shear Zone. Emile Argand Conference on Alpine Geological Studies 2019. Sion, Switzerland, 4 pp.

Ballèvre, M., Merle, O., 1993. The Combin Fault : compressional reactivation of a Late Cretaceous-Early Tertiary detachment fault in the Western Alps. Schweizerische Mineralogische Und Petrographische Mitteilungen 73, 205–227. https://doi.org/https://doi.org/10/gfsjrz

Baretti, M., 1881. Apercu géologique sur la Chaine du Mont Blanc en rapport avec le traject probable d'un tunnel pour la nouvelle ligne de chemin de fer. Mem. Comité Local d'Aoste Promoteur de La Percée Du Mont Blanc, J. Candeletti Editeur-Imprimeur, Turin 38 pp.

Bearth, P., 1967. Die Ophiolithe der Zone von Zermatt-Saas Fee. Beiträge Zur Geologischen Karte Der Schweiz 132, 130 pp.

Beltrando, M., Frasca, G., Compagnoni, R., Vitale-Brovarone, A., 2012. The Valaisan controversy revisited: Multi-stage folding of a Mesozoic hyper-extended margin in the Petit St. Bernard pass area (Western Alps). Tectonophysics 579, 17–36. https://doi.org/10.1016/j.tecto.2012.02.010

Bergomi, M.A., Dal Piaz, G. V, Malusà, M.G., Monopoli, B., Tunesi, A., 2017. The Grand St Bernard-Briançonnais Nappe System and the Paleozoic Inheritance of the Western Alps Unraveled by Zircon U-Pb Dating. Tectonics 36, 2950–2972. https://doi.org/10.1002/2017TC004621

Bertrand, J.M., Aillères, L., Gasquet, D., 1996. The Pennine Front zone in Savoie (Western Alps), a review and new interpretations from the Zone Houillère Briançonnaise. Eclogae Geologicae Helvetiae 89, 298–320.

Bigi, G., Castellarin, A., Coli, M., Dal Piaz, G. V, Sartori, R., Scandone, P., Vai, G.B., 1990. Structural Model of Italy 1:500.000, Sheet 1, C.N.R. Progetto Geodinamica, SELCA Firenze. SELCA, Firenze.

Bistacchi, A., Dal Piaz, G., Massironi, M., Zattin, M., Balestrieri, M., 2001. The Aosta–Ranzola extensional fault system and Oligocene–Present evolution of the Austroalpine–Penninic wedge in the northwestern Alps. International Journal of Earth Sciences 90, 654–667. https://doi.org/10.1007/s005310000178

Bistacchi, A., Eva, E., Massironi, M., Solarino, S., 2000. Miocene to Present kinematics of the NW-Alps: evidences from remote sensing, structural analysis, seismotectonics and thermochronology. Journal of Geodynamics 30, 205–228. https://doi.org/https://doi.org/10.1016/S0264-3707(99)00034-4

Bistacchi, A., Massironi, M., 2000. Post-nappe brittle tectonics and kinematic evolution of the north-western Alps: an integrated approach. Tectonophysics 327, 267–292. https://doi.org/10.1016/S0040-1951(00)00206-7

Bistacchi, A., Massironi, M., Dal Piaz, Giorgio V, Dal Piaz, Giovanni, Monopoli, B., Schiavo, A., Toffolon, G., 2008. 3D fold and fault reconstruction with an uncertainty model: An example from an Alpine tunnel case study. Computers and Geosciences 34, 351–372. https://doi.org/10.1016/j.cageo.2007.04.002

Bond, C.E., 2015. Uncertainty in structural interpretation: Lessons to be learnt. Journal of Structural Geology 74, 185–200. https://doi.org/10.1016/j.jsg.2015.03.003

Bonetto, F., Dal Piaz, G.V., de Giusti, F., Massironi, M., Monopoli, B., Schiavo, A., 2010. Carta

geologica della Valle d'Aosta alla scala 1:100.000. Regione Autonoma Valle d'Aosta, Dipartimento Difesa Del Suolo e Risorse Idriche, Tipografia Valdostana 23 pp.

Borradaile, G., 2003. Statistics of Earth Science Data. Springer Berlin Heidelberg, Berlin, Heidelberg. https://doi.org/10.1007/978-3-662-05223-5

Burri, M., 1983. Description geologique du front du St. Bernard dans les Vallees de Bagnes et d'Entremont. Eclogae Geologicae Helvetiae 76, 469–490.

Burri, M., Allimann, M., Chessex, R., Dal Piaz, G. V, Della Valle, G., Du Bois, L., Gouffon, Y., Guermani, A., Hagen, T., Krummenacher, D., Looser, M.O., 1998. Feuille 1346 Chanrion avec partie nord de la feuille 1366 Mont Vélan, Atlas géologique de la Suisse 1:25.000. Service hydrologique et géologique national, Berne.

Burri, M., Marro, C., 1993. Feuille 1345 Orsières, Atlas géologique de la Suisse 1:25.000. Service hydrologique et géologique national, Berne.

Caby, R., 1981. Le Mésozoïque de la zone du Combin en Val d'Aoste (Alpes Graies): Imbrications tectoniques entre séries issues des domaines pennique, austroalpin et océanique. Gèologie Alpine 57, 5–13.

Caby, R., 1968. Contribution à l'étude structurale des Alpes Occidentales: Subdivisions stratigraphiques et structure de la zone du Grand-Saint-Bernard dans la partie sud du Val d'Aoste (Italie). Géologie Alpine 44, 95–111.

Calcagno, P., Chilès, J.P., Courrioux, G., Guillen, A., 2008. Geological modelling from field data and geological knowledge. Part I. Modelling method coupling 3D potential-field interpolation and geological rules. Physics of the Earth and Planetary Interiors 171, 147–157. https://doi.org/10.1016/j.pepi.2008.06.013

Canepa, M., Castelletto, M., Cesare, B., Martin, S., Zaggia, L., 1990. The Austroapine Mont Mary nappe (Italian Western Alps). Memorie Scienze Geologiche 42, 1–17.

Carmichael, T., Ailleres, L., 2016. Method and analysis for the upscaling of structural data. Journal of Structural Geology 83, 121–133. https://doi.org/10.1016/j.jsg.2015.09.002

Carr, J.C., Beatson, R.K., Cherrie, J.B., Mitchell, T.J., Fright, W.R., McCallum, B.C., Evans, T.R., 2001. Reconstruction and representation of 3D objects with radial basis functions. Proceedings of the 28th Annual Conference on Computer Graphics and Interactive Techniques. Association for Computing Machinery, 67–76. https://doi.org/10.1145/383259.383266

Cartwright, I., Barnicoat, A.C., 2002. Petrology, geochronology, and tectonics of shear zones in the Zermatt-Saas and Combin zones of the Western Alps. Journal of Metamorphic Geology 20, 263–281. https://doi.org/10.1046/j.0263-4929.2001.00366.x

Caumon, G., 2010. Towards stochastic time-varying geological modeling. Math Geosci 42, 555–569. https://doi.org/10.1007/s11004-010-9280-y

Caumon, G., Collon-Drouaillet, P., Le Carlier de Veslud, C., Viseur, S., Sausse, J., 2009. Surface-Based 3D Modeling of Geological Structures. Mathematical Geosciences 41, 927–945. https://doi.org/10.1007/s11004-009-9244-2

Caumon, G., Gray, G., Antoine, C., Titeux, M.O., 2013. Three-dimensional implicit stratigraphic model building from remote sensing data on tetrahedral meshes: Theory and application to a regional model of la Popa Basin, NE Mexico. IEEE Transactions on Geoscience and Remote Sensing 51, 1613–1621. https://doi.org/10.1109/TGRS.2012.2207727

Caumon, G., Lepage, F., Sword, C.H., Mallet, J.L., 2004. Building and editing a sealed geological model. Mathematical Geology 36, 405–424.

https://doi.org/10.1023/B:MATG.0000029297.18098.8a

Ceriani, S., Fügenschuh, B., Schmid, S.M., 2001. Multi-stage thrusting at the" Penninic Front" in the Western Alps between Mont Blanc and Pelvoux massifs. Int J Earth Sci 90, 685–702. https://doi.org/10.1007/s005310000188

Cita, B.M., 1953. Studi geologici sulla Valle Ferret italiana. Bollettino Del Servizio Geologico Italiano 75, 65–172.

Compagnoni, R., 2003. HP metamorphic belt of the western Alps. Episodes 26, 200–204. https://doi.org/10.18814/EPIIUGS/2003/V26I3/008

Compagnoni, R., Dal Piaz, G. V, Hunziker, J.C., Gosso, G., Lombardo, B., Williamns, P.F., 1977. The Sesia-Lanzo zone, a slice of continental crust with Alpine high pressure-low temperature assem-blages in the Western Italian Alps. Rendiconti Della Società Italiana Di Mineralogia e Petrologia 33, 281–334.

Cortiana, G., Dal Piaz, G. V, Del Moro, A., Hunziker, J.C., Martin, S., 1998. 40Ar-39Ar and Rb-Sr dating on the Pillonet klippe and frontal Sesia-Lanzo zone in the Ayas valley and evolution of the western Austroalpine nappe stack. Memorie Scienze Geologiche 50, 177–194.

Dal Piaz, G., Cortiana, G., Del Moro, A., Martin, S., Pennacchioni, G., Tartarotti, P., 2001. Tertiary age and paleostructural inferences of the eclogitic imprint in the Austroalpine outliers and Zermatt–Saas ophiolite, western Alps. International Journal of Earth Sciences 90, 668–684. https://doi.org/10.1007/s005310000177

Dal Piaz, G.V., 2001. Geology of the Monte Rosa massif: historical review and personal comments. Schweizerische Mineralogische Und Petrographische Mitteilungen 81, 273–303. https://doi.org/https://doi.org/10.5169/SEALS-61694

Dal Piaz, G.V., 1976. Il lembo di ricoprimento del Pillonet: falda della Dent Blanche nelle Alpi occidentali. Memorie Istituti Geologia Mineralogia Università Di Padova 31, 60 pp.

Dal Piaz, G.V., 1965. La formazione mesozoica dei calcescisti con pietre verdi fra la Valsesia e la Valtournanche ed i suoi rapporti strutturali con il ricoprimento del Monte Rosa e con la Zona SesiaLanzo. Bollettino Della Società Geologica Italiana 84, 67–104.

Dal Piaz, G.V., Bistacchi, A., Gianotti, F., Monopoli, B., Passeri, L., Schiavo, A., Bertolo, D., Bonetto, F., Ciarapica, G., Dal Piaz, G., Gouffon, Y., Massironi, M., Ratto, S., Toffolon, G., 2016. Foglio 070 Cervino e Note Illustrative. Carta Geologica d'Italia Alla Scala 1:50.000, ISPRA, Regione Autonoma Valle d'Aosta 432 pp.

Dal Piaz, G.V., Gianotti, F., Monopoli, B., Pennacchioni, G., Tartarotti, P., Schiavo, A., Carraro, F., Bistacchi, A., Massironi, M., Martin, S., Ratto, S., 2010. Foglio 091 Chatillon e Note Illustrative. Carta Geologica d'Italia Alla Scala 1:50.000, ISPRA, Regione Autonoma Valle d'Aosta 152 pp.

Dal Piaz, G. V, 2004. From the European continental margin to the Mesozoic Tethyan ocean: A geological map of the upper Ayas valley (Western Alps). In: Pasquarè, G., Venturini, C. (Eds.), Mapping Geology in Italy. APAT-Dip. Difesa del Suolo-Servizio Geolologico d'Italia, S.E.L.C.A., Firenze, 265–272.

Dal Piaz, G. V, 1999. The Austroalpine-Piedmont nappe stack and the puzzle of Alpine Tethys. Memorie Scienze Geologiche 53, 153–162.

Dal Piaz, G. V, Bistacchi, A., Massironi, M., 2003. Geological outline of the Alps. Episodes Journal of International Geoscience 26, 175–180. https://doi.org/10.18814/EPIIUGS/2003/V26I3/004

Dal Piaz, G. V, Sacchi, R., 1969. Osservazioni geologiche sul lembo di ricoprimento del Pillonet

(Dent Blanche l.s.). Memorie Scienze Geologiche 8, 835–846.

de Kemp, E.A., 2000. 3-D visualization of structural field data: Examples from the Archean Caopatina Formation, Abitibi greenstone belt, Québec, Canada. Computers and Geosciences 26, 509–530. https://doi.org/10.1016/S0098-3004(99)00142-9

De La Varga, M., Schaaf, A., Wellmann, F., 2019. GemPy 1.0: Open-source stochastic geological modeling and inversion. Geoscientific Model Development 12, 1–32. https://doi.org/10.5194/gmd-12-1-2019

Elter, G., 1960. La zona Pennidica dell'alta e media Valle d'Aosta con carta tettonica al 1:100.000. Memorie Istituti Geologia Mineralogia Università Di Padova 22, 113 pp.

Elter, G., Elter, P., 1965. Carta geologica della regione del Piccolo S. Bernardo (versante italia-no). Note Illustrative, Memorie Istituti Geologia Mineralogia Università Di Padova 25, 53 pp.

Ernst, W.G., Dal Piaz, G. V, 1978. Mineral parageneses of eclogitic rocks and related mafic schists of the Piemonte ophiolite nappe, Breuil-St. Jacques area, Italian Western Alps. American Mineralogist 63, 621–640.

Escher, A., Masson, H., Steck, A., 1988. Coupes géologiques des Alpes occidentales suisses. Mémoires de Géologie de l'Université de Lausanne 2, 5–11.

Frank, T., Tertois, A.L., Mallet, J.L., 2007. 3D-reconstruction of complex geological interfaces from irregularly distributed and noisy point data. Computers and Geosciences 33, 932–943. https://doi.org/10.1016/j.cageo.2006.11.014

Frey, M., Hunziker, J.C., Frank, W., Bocquet, J., Dal Piaz, G.V., Jäger, E., Niggli, E., 1974. Alpine metamorphism of the Alps: a review. Schweiz. Mineral. Petrogr. Mitt. 54, 247–290.

Frezzotti, M.L., Huizenga, J.M., Compagnoni, R., Selverstone, J., 2014. Diamond formation by carbon saturation in C-O-H fluids during cold subduction of oceanic lithosphere. Geochimica et Cosmochimica Acta 143, 68–86. https://doi.org/10.1016/J.GCA.2013.12.022

Frodeman, R., 1995. Geological reasoning: Geology as an interpretive and historical science. Geological Society of America Bulletin 107, 960–0968. https://doi.org/10.1130/0016-7606(1995)107<0960:GRGAAI>2.3.CO;2

Gardien, V., Reusser, E., Marquer, D., 1994. Pre-Alpine metamorphic evolution of the gneisses from the Valpelline Series (Western Alps, Italy). Schweizerische Mineralogische Und Petrographische Mitteilungen 74, 489–502.

Giraud, J., Caumon, G., Grose, L., Ogarko, V., Cupillard, P., 2023. Integration of automatic implicit geological modelling in deterministic geophysical inversion. EGUsphere Preprint. https://doi.org/10.5194/egusphere-2023-129

Giusti, F. De, Dal Piaz, G. V, Massironi, M., Schiavo, A., 2003. Carta geotettonica della Valle d'Aosta. Memorie Scienze Geologiche 55, 129–149.

Godefroy, G., Caumon, G., Ford, M., Laurent, G., Jackson, C.A.-L., 2018. A parametric fault displacement model to introduce kinematic control into modeling faults from sparse data. Interpretation 6, B1–B13. https://doi.org/10.1190/INT-2017-0059.1

Gouffon, Y., 1993. Géologie de la" nappe" du Grand St-Bernard entre la Doire Baltée et la frontière suisse (Vallée d'Aoste-Italie). Mémoires de Géologie de l'Université de Lausanne 12, 1–147.

Grose, L., Ailleres, L., Laurent, G., Jessell, M., 2021. LoopStructural 1.0: Time-aware geological modelling. Geoscientific Model Development 14, 3915–3937. https://doi.org/10.5194/gmd-14-3915-2021

Grose, L., Laurent, G., Aillères, L., Armit, R., Jessell, M., Caumon, G., 2017. Structural data constraints for implicit modeling of folds. Journal of Structural Geology 104, 80–92. https://doi.org/10.1016/j.jsg.2017.09.013

Guillen, A., Calcagno, P., Courrioux, G., Joly, A., Ledru, P., 2008. Geological modelling from field data and geological knowledge. Part II. Modelling validation using gravity and magnetic data inversion. Physics of the Earth and Planetary Interiors 171, 158–169. https://doi.org/10.1016/j.pepi.2008.06.014

Hassen, I., Gibson, H., Hamzaoui-Azaza, F., Negro, F., Rachid, K., Bouhlila, R., 2016. 3D geological modeling of the Kasserine Aquifer System, Central Tunisia: New insights into aquifer-geometry and interconnections for a better assessment of groundwater resources. Journal of Hydrology 539, 223–236. https://doi.org/10.1016/J.JHYDROL.2016.05.034

Hillier, M., de Kemp, E., Schetselaar, E., 2013. 3D form line construction by structural field interpolation (SFI) of geologic strike and dip observations. Journal of Structural Geology 51, 167–179. https://doi.org/https://doi.org/10.1016/j.jsg.2013.01.012

Hillier, M.J., Schetselaar, E.M., de Kemp, E.A., Perron, G., 2014. Three-Dimensional Modelling of Geological Surfaces Using Generalized Interpolation with Radial Basis Functions. Mathematical Geosciences 46, 931–953. https://doi.org/10.1007/s11004-014-9540-3

Houlding, S.W., 1994. The Geological Characterization Process. 3D Geoscience Modeling. Springer Berlin Heidelberg, Berlin, Heidelberg, 7–26. https://doi.org/10.1007/978-3-642-79012-6_2

Irakarama, M., Laurent, G., Renaudeau, J., Caumon, G., 2018. Finite Difference Implicit Modeling of Geological Structures. 80th EAGE Conference and Exhibition 2018: Opportunities Presented by the Energy Transition. European Association of Geoscientists and Engineers, EAGE, 1–5. https://doi.org/10.3997/2214-4609.201800794

Irakarama, M., Thierry-Coudon, M., Zakari, M., Caumon, G., 2022. Finite Element Implicit 3D Subsurface Structural Modeling. Computer-Aided Design 149, 103267. https://doi.org/10.1016/j.cad.2022.103267

Jessell, M., Aillères, L., Kemp, E. de, Lindsay, M., Wellmann, F., Hillier, M., Laurent, G., Carmichael, T., Martin, R., 2014. Next Generation Three-Dimensional Geologic Modeling and Inversion. Building Exploration Capability for the 21st Century. Society of Economic Geologists. https://doi.org/10.5382/SP.18.13

Jessell, M., Ogarko, V., de Rose, Y., Lindsay, M., Joshi, R., Piechocka, A., Grose, L., de la Varga, M., Ailleres, L., Pirot, G., 2021. Automated geological map deconstruction for 3D model construction using map2loop 1.0 and map2model 1.0. Geoscientific Model Development 14, 5063–5092. https://doi.org/10.5194/gmd-14-5063-2021

Jessell, M.W., Ailleres, L., de Kemp, E.A., 2010. Towards an integrated inversion of geoscientific data: What price of geology? Tectonophysics 490, 294–306. https://doi.org/10.1016/J.TECTO.2010.05.020

Kaufmann, O., Martin, T., 2009. Reprint of "3D geological modelling from boreholes, cross-sections and geological maps, application over former natural gas storages in coal mines" [Comput. Geosci. 34 (2008) 278-290]. Computers and Geosciences 35, 70–82. https://doi.org/10.1016/S0098-3004(08)00227-6

Kroeger, K.F., Crutchley, G.J., Kellett, R., Barnes, P.M., 2019. A 3-D Model of Gas Generation, Migration, and Gas Hydrate Formation at a Young Convergent Margin (Hikurangi Margin, New Zealand). Geochemistry, Geophysics, Geosystems 20, 5126–5147.

https://doi.org/10.1029/2019GC008275

Lajaunie, C., Courrioux, G., Manuel, L., 1997. Foliation fields and 3D cartography in geology: Principles of a method based on potential interpolation. Mathematical Geology 29, 571–584. https://doi.org/10.1007/BF02775087

Lapen, T.J., Johnson, C.M., Baumgartner, L.P., Dal Piaz, G. V, Skora, S., Beard, B.L., 2007. Coupling of oceanic and continental crust during Eocene eclogite-facies metamorphism: evidence from the Monte Rosa nappe, western Alps. Contributions to Mineralogy and Petrology 153, 139–157. https://doi.org/10.1007/s00410-006-0144-x

Lardeaux, J.M., Spalla, M.I., 1991. From granulites to eclogites in the Sesia zone (Italian Western Alps): a record of the opening and closure of the Piedmont ocean. Journal of Metamorphic Geology 9, 35–59. https://doi.org/10.1111/j.1525-1314.1991.tb00503.x

Laurent, G., 2016. Iterative Thickness Regularization of Stratigraphic Layers in Discrete Implicit Modeling. Mathematical Geosciences 48, 811–833. https://doi.org/10.1007/s11004-016-9637-y

Laurent, G., Ailleres, L., Grose, L., Caumon, G., Jessell, M., Armit, R., 2016. Implicit modeling of folds and overprinting deformation. Earth and Planetary Science Letters 456, 26–38. https://doi.org/10.1016/j.epsl.2016.09.040

Laurent, G., Caumon, G., Bouziat, A., Jessell, M., 2013. A parametric method to model 3D displacements around faults with volumetric vector fields. Tectonophysics 590, 83–93. https://doi.org/10.1016/j.tecto.2013.01.015

Liang, Z., Wellmann, F., Ghattas, O., 2023. Uncertainty quantification of geologic model parameters in 3D gravity inversion by Hessian-informed Markov chain Monte Carlo. Geophysics 88, G1–G18. https://doi.org/10.1190/geo2021-0728.1

Loprieno, A., Bousquet, R., Bucher, S., Ceriani, S., Dalla Torre, F.H., Fügenschuh, B., Schmid, S.M., 2011. The Valais units in Savoy (France): a key area for understanding the palaeogeography and the tectonic evolution of the Western Alps. International Journal of Earth Sciences 100, 963–992. https://doi.org/https://doi.org/10.1007/s00531-010-0595-1

Mallet, J.-L., 2014. Elements of Mathematical Sedimentary Geology: the GeoChron Model. EAGE Publications 374 pp. https://doi.org/10.3997/9789462820081

Mallet, J.-L., 2004. Space – Time Mathematical Framework for Sedimentary Geology. Math. Geol. 36, 1–32.

Malusà, M.G., Polino, R., Martin, S., 2005. The Gran San Bernardo nappe in the Aosta valley (western Alps): a composite stack of distinct continental crust units. Bulletin de La Société Géologique de France 176, 417–431. https://doi.org/10.2113/176.5.417

Manzotti, P., Ballèvre, M., Dal Piaz, G.V., 2017. Continental gabbros in the Dent Blanche Tectonic System (Western Alps): from the pre-Alpine crustal structure of the Adriatic palaeo-margin to the geometry of an alleged subduction interface. Journal of the Geological Society 174, 541–556. https://doi.org/10.1144/jgs2016-071

Manzotti, P., Ballèvre, M., Pitra, P., Schiavi, F., 2021. Missing lawsonite and aragonite found: P–T and fluid composition in meta-marls from the Combin Zone (Western Alps). Contributions to Mineralogy and Petrology 176, 60. https://doi.org/10.1007/s00410-021-01818-0

Manzotti, P., Ballèvre, M., Zucali, M., Robyr, M., Engi, M., 2014a. The tectonometamorphic evolution of the Sesia-Dent Blanche nappes (internal Western Alps): review and synthesis. Swiss Journal of Geosciences 107, 309–336. https://doi.org/10.1007/s00015-014-0172-x

Manzotti, P., Zucali, M., Ballèvre, M., Robyr, M., Engi, M., 2014b. Geometry and kinematics of the Roisan-Cignana Shear Zone, and the orogenic evolution of the Dent Blanche Tectonic System (Western Alps). Swiss Journal of Geosciences 107, 23–47. https://doi.org/10.1007/s00015-014-0157-9

Maxelon, M., Mancktelow, N.S., 2005. Three-dimensional geometry and tectonostratigraphy of the Pennine zone, Central Alps, Switzerland and Northern Italy. Earth-Science Reviews 71, 171–227. https://doi.org/10.1016/j.earscirev.2005.01.003

Maxelon, M., Renard, P., Courrioux, G., Brändli, M., Mancktelow, N., 2009. A workflow to facilitate three-dimensional geometrical modelling of complex poly-deformed geological units. Computers & Geosciences 35, 644–658. https://doi.org/10.1016/j.cageo.2008.06.005

Milicich, S.D., Pearson-Grant, S.C., Alcaraz, S., White, P.A., Tschritter, C., 2018. 3D Geological modelling of the Taupo Volcanic Zone as a foundation for a geothermal reservoir model. New Zealand Journal of Geology and Geophysics 61, 79–95. https://doi.org/10.1080/00288306.2017.1407346

Milnes, A.G., Greller, M., Müller, R., 1981. Sequence and style of major post-nappe structures, Simplon—Pennine Alps. Journal of Structural Geology 3, 411–420. https://doi.org/10.1016/0191-8141(81)90041-9

Nicolas, A., Polino, R., Hirn, A., Nicolich, R., 1990. ECORS-CROP traverse and deep structure of the western Alps: a synthesis. Mem. Soc. Geol. Fr 156, 15–27.

Pantet, A., Epard, J.L., Masson, H., 2020. Mimicking Alpine thrusts by passive deformation of synsedimentary normal faults: a record of the Jurassic extension of the European margin (Mont Fort nappe, Pennine Alps). Swiss Journal of Geosciences 113, 1–25. https://doi.org/https://doi.org/10.1186/s00015-020-00366-2

Perello, P., Gianotti, F., Monopoli, B., Carraro, F., Venturini, G., Fontan, D., Schiavo, A., Bonetto, F., 2011. Foglio 089 Courmayeur e Note Illustrative. Carta Geologica d'Italia Alla Scala 1:50.000, ISPRA, Regione Autonoma Valle d'Aosta 152 pp.

Perrin, M., Zhu, B., Rainaud, J.F., Schneider, S., 2005. Knowledge-driven applications for geological modeling. Journal of Petroleum Science and Engineering 47, 89–104. https://doi.org/10.1016/J.PETROL.2004.11.010

Pfiffner, O.A., Lehener, P., Heitzmann, P., Mueller, S., Steck, A., 1997. Deep Structure of the Swiss Alps: Results from NRP 20. Birkhäuser, Basel.

Philippon, M., de Veslud, C.L.C., Gueydan, F., Brun, J.P., Caumon, G., 2015. 3D geometrical modelling of post-foliation deformations in metamorphic terrains (Syros, Cyclades, Greece). Journal of Structural Geology 78, 134–148. https://doi.org/10.1016/j.jsg.2015.07.002

Pizzella, L., Alais; R., Lopez, S., Freulon, X., Rivoirard, J., 2022. Taking better advantage of foldfold Axis data to characterize anisotropy of complex folded structures in the implicit modeling framework. Mathematical Geosciences 54, 95-130, https://doi.org/10.1007/s11004-021-09950-0

Polino, R., Malusà, M.G., S, M., Carraro, F., Gianotti, F., Bonetto, F., Perello, P., Schiavo, A., Gouffon, Y., 2015. Foglio 090 Aosta e Note Illustrative. Carta Geologica d'Italia Alla Scala 1:50.000, ISPRA, Regione Autonoma Valle d'Aosta 144 pp.

Reddy, S.M., Wheeler, J., Butler, R.W.H., Cliff, R.A., Freeman, S., Inger, S., Pickles, C., Kelley, S.P., 2003. Kinematic reworking and exhumation within the convergent Alpine Orogen. Tectonophysics 365, 77–102. https://doi.org/10.1016/S0040-1951(03)00017-9

Reinecke, T., 1991. Very-high-pressure metamorphism and uplift of coesite-bearing metasediments from the Zermatt-Saas zone, Western Alps. European Journal of Mineralogy 3, 7–18.

Renaudeau, J., Malvesin, E., Maerten, F., Caumon, G., 2019. Implicit Structural Modeling by Minimization of the Bending Energy with Moving Least Squares Functions. Mathematical Geosciences 51, 693–724. https://doi.org/10.1007/s11004-019-09789-6

Sartori, M., Gouffon, Y., Marthaler, M., 2006. Harmonisation et définition des unités lithostratigraphiques briançonnaises dans les nappes penniques du Valais. Eclogae Geologicae Helvetiae 99, 363–407.

Sides, E.J., 1997. Geological modelling of mineral deposits for prediction in mining. Geologische Rundschau 86, 342–353. https://doi.org/https://doi.org/10.1007/s005310050145

Soldo, L., Arienti, G., Bistacchi, A., Mezzanzanica, M., Regondi, L., Pizzarotti, E.M., 2022. Modellazione Geologica digitale e sua integrazione nelle moderne metodologie di progetto di opere infrastrutturali - Digital Geological Modelling within the modern infrastructure design methodologies. Gallerie e Grandi Opere Sotterranee 142, 27–40.

Steck, A., Masson, H., Robyr, M., 2015. Tectonics of the Monte Rosa and surrounding nappes (Switzerland and Italy): Tertiary phases of subduction, thrusting and folding in the Pennine Alps. Swiss Journal of Geosciences 108, 3–34. https://doi.org/10.1007/s00015-015-0188-x

Sue, C., Delacou, B., Champagnac, J.D., Allanic, C., Tricart, P., Burkhard, M., 2007. Extensional neotectonics around the bend of the Western/Central Alps: An overview. International Journal of Earth Sciences 96, 1101–1129. https://doi.org/10.1007/S00531-007-0181-3

Thanh, H.V., Sugai, Y., Nguele, R., Sasaki, K., 2019. Integrated workflow in 3D geological model construction for evaluation of CO2 storage capacity of a fractured basement reservoir in Cuu Long Basin, Vietnam. International Journal of Greenhouse Gas Control 90, 102826. https://doi.org/10.1016/J.IJGGC.2019.102826

Thornton, J.M., Mariethoz, G., Brunner, P., 2018. A 3D geological model of a structurally complex alpine region as a basis for interdisciplinary research. Scientific Data 5, 180238. https://doi.org/10.1038/sdata.2018.238

Trümpy, R., 1955. Remarques sur la correlation des unites penniques externes entre la Savoie et le Valais et sur l'origine des nappes pre´alpines. Bulletin De La Societe Geologique De France 5, 217–231.

Trümpy, R., 1954. La zone de Sion-Courmayeur dans le haut Val Ferret valaisan. Eclogae Geologicae Helvetiae 47, 317–359.

Trümpy, R., 1952. Sur les racines helvétiques et les «Schistes lustrés» entre le Rhône et la Vallée de Bagnes (Région de la Pierre Avoi). Eclogae Geologicae Helvetiae 44, 338–347.

Vollgger, S.A., Cruden, A.R., Ailleres, L., Cowan, E.J., 2015. Regional dome evolution and its control on ore-grade distribution: Insights from 3D implicit modelling of the Navachab gold deposit, Namibia. Ore Geology Reviews 69, 268–284. https://doi.org/https://doi.org/10.1016/j.oregeorev.2015.02.020

Vollmer, F.W., 1995. C program for automatic contouring of spherical orientation data using a modified Kamb method. Computers and Geosciences 21, 31–49. https://doi.org/10.1016/0098-3004(94)00058-3

von Raumer, J.F., Bussy, F., 2004. Mont Blanc and Aiguilles Rouges; geology of their polymetamorphic basement (External massifs, Western Alps, France-Switzerland). Mémoires de Géologie (Lausanne) 42, 1–203.

Wellmann, F., Caumon, G., 2018. 3-D Structural geological models: Concepts, methods, and uncertainties. Advances in Geophysics 59, 1–121. https://doi.org/10.1016/bs.agph.2018.09.001

Wheeler, J., Butler, R.W.H., 1993. Evidence for extension in the western Alpine orogen: the contact between the oceanic Piemonte and overlying continental Sesia units. Earth and Planetary Science Letters 117, 457–474. https://doi.org/10.1016/0012-821X(93)90097-S

Xiong, Z., Guo, J., Xia, Y., Lu, H., Wang, M., Shi, S., 2018. A 3D Multi-scale geology modeling method for tunnel engineering risk assessment. Tunnelling and Underground Space Technology 73, 71–81. https://doi.org/10.1016/J.TUST.2017.12.003

Zanchi, A., Francesca, S., Stefano, Z., Simone, S., Graziano, G., 2009. 3D reconstruction of complex geological bodies: Examples from the Alps. Computers and Geosciences 35, 49–69. https://doi.org/10.1016/j.cageo.2007.09.003